Lawrence Berkeley Laboratory
UNIVERSITY OF CALIFORNIA

Physics Division

Submitted for publication

THE TeV PHYSICS OF STRONGLY INTERACTING W's and Z's

M.S. Chanowitz and M.K. Gaillard

May 1985

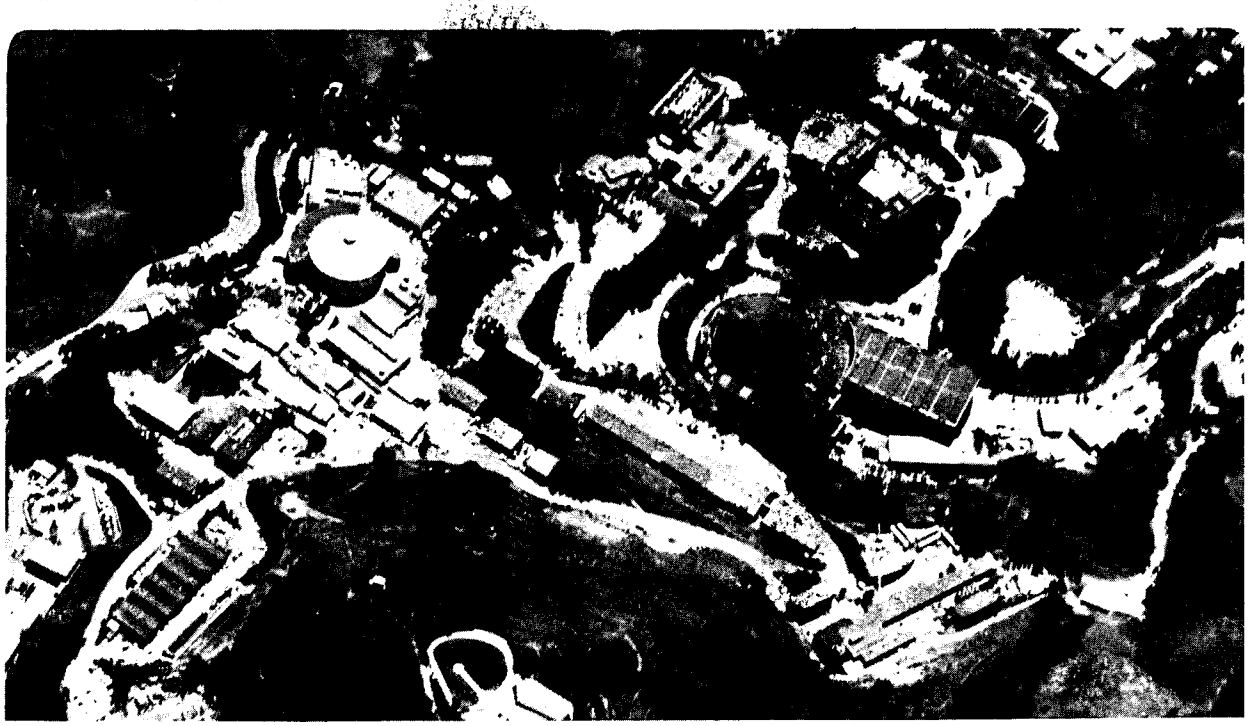

Prepared for the U.S. Department of Energy under Contract DE-AC03-76SF00098

DISCLAIMER

May 1985

LBL-19470
UCB-PTH-85/19

THE TeV PHYSICS OF STRONGLY INTERACTING W's AND Z's *

Michael S. Chanowitz

Lawrence Berkeley Laboratory
University of California
Berkeley, California 94720

Mary K. Gaillard

Lawrence Berkeley Laboratory
and
Department of Physics
University of California
Berkeley, California 94720

*This work was supported by the Director, Office of Energy Research, Office of High Energy and Nuclear Physics, Division of High Energy Physics of the U.S. Department of Energy under Contract DE-AC03-76SF00098 and National Science Foundation under Research Grant No. PHY-84-06608.

ABSTRACT

There are two possibilities for electroweak symmetry breaking: either there is a scalar particle much lighter than 1 TeV or the longitudinal components of W and Z bosons interact strongly at center of mass energies of order 1 TeV or more. We study the general signatures of a strongly interacting W, Z system and conclude that these two possibilities can be unambiguously distinguished by a hadron collider facility capable of observing the enhanced production of WW, WZ and ZZ pairs that will occur if W's and Z's have strong interactions. Detection of the enhanced signal over background requires hadron collisions at a center of mass energy of order $\sqrt{s} = 40\ TeV$ and an integrated luminosity of order $10^{40} cm^{-2}$. With these parameters we predict 3800 to 6000 gauge boson pairs satisfying cuts for which only 2600 pairs would be produced in the absence of strong interactions.

As our results draw on the global chiral $SU(2)$ symmetry of the scalar sector of the standard $SU(2) \times U(1)$ model, we give an extended proof, to all orders in the generalized renormalizable gauge, that high energy amplitudes of longitudinal W's and Z's are well approximated by amplitudes of the corresponding unphysical scalars. The results are applicable to the broad class of strong interaction models that admit a global chiral $SU(2)$ symmetry.

1. Introduction

Experiments at the proposed Superconducting Super Collider will study hard collisions with effective center of mass energies up to several TeV, and will provide a copious source of the intermediate vector bosons, $W^{\pm}$ and Z, of the electroweak interactions. Unless there is a Higgs boson appreciably lighter than 1 TeV, very general arguments require[1,2] longitudinally polarized W's and Z's to have strong interactions with one another in this energy range. We concentrate in this paper on the most general experimental signals for strongly coupled W's and Z's. We find that a collider with specifications like those proposed for the SSC — $\sqrt{s} = 0(40)TeV$ and $\mathcal{L} = 0(10^{33})cm.^{-2}sec.^{-1}$ — is needed to observe these signals.

Unless a Higgs particle is light enough to detect at LEP or SLC, such a collider cannot fail to make a fundamental contribution to our understanding of the origin of electroweak symmetry breaking. If the signal for strongly interacting W's and Z's were not observed, it would provide the strongest possible motivation for a redoubled effort to search for a light Higgs sector. For example a standard model Higgs in the mass window 85 $GeV \leq m_H \leq 2M_W$ would almost surely have escaped detection as it would be above the reach of LEP II and lacking the WW and ZZ decay modes that allow detection above background in hadron colliders.[3] If on the other hand the signal for strongly interacting W's and Z's were seen, the SSC would be our unique window on a new force and a new spectrum of particles. As we will show, less ambitious hadron colliders would have no possibility of studying these phenomena.

If longitudinal W's and Z's are strongly interacting, their physics is governed by the dynamics of the mechanism which breaks the gauge symmetry. For example, technicolor models[4] predict a specific spectrum of W, Z resonance states, analogous to the pion resonances of QCD, while the strong W, Z interaction limit of ultracolor[5] models have a rather different spectrum. Another example is a strongly coupled scalar field theory, in which the scalars are either elementary (as in the standard model) or, more likely, composite at a scale much smaller than the $10^{-16}cm.$ scale of electroweak symmetry breaking. In this case, except for what might be dictated by symmetry considerations, we have little idea of the nature of the spectrum.

There are however predictions, based on current algebra and $PCAC$, which characterize a large class of models of strongly coupled W, Z systems. In a recent paper[6] we emphasized multiple W and Z production as a signal for symmetry breaking by new strong interactions. We investigated mechanisms for the production in

pp collisions of two or more longitudinally polarized gauge bosons, W_L, Z_L, since it is these components that may interact strongly, and we estimated W_L and Z_L multiplicities. In this paper we present a more complete discussion of these production mechanisms.

The most prominent signal for strongly interacting W's and Z's is the production of gauge boson pairs by the double bremstrahlung mechanism of Figure (1), first discussed in the context of Higgs production.[7] For our purposes the important point is that Figure (1) is a negligible source of gauge boson pairs if the rescattering amplitude $T(V_1V_2 \to V_1'V_2')$ is only of electroweak strength. In this case, Figure (1) is suppressed by $0(\alpha_W^2)$ in rate relative to $\bar{q}q$ annihilation shown in Figure (2). But if T is of strong interaction strength, then the double bremstrahlung mechanism dominates $\bar{q}q$ annihilation for large mass boson pairs produced away from the forward direction. By counting large mass, nonforward boson pairs, we can learn whether W_L and Z_L have strong interactions.

To estimate the strong interaction amplitude $T(V_1V_2 \to V_1'V_2')$ and other relevant strong interaction amplitudes, such as 2 bosons $\to$ 4 bosons, two steps are involved. The first is to associate $S-$matrix elements of external longitudinally polarized vector bosons, $W_L^{\pm}, Z_L$, with $S-$matrix elements of the corresponding unphysical scalar bosons w and z which are "eaten" to make W and Z massive. This equivalence has been claimed[2,8,9] to hold in Higgs theories to order $(m_{W,Z}/E_{W,Z})$ where $E_{W,Z}$ are the energies of the external bosons. Since the previous derivations[2,8,9] are not sufficiently general for our purposes, we devote Section 2 of this paper to an extension of the equivalence theorem in a general R_ξ gauge and to all orders in perturbation theory. That section is rather technical and can be omitted by the reader primarily interested in the phenomenology of strongly interacting W's and Z's.

The second step in our program is to use current algebra and $PCAC$ to derive low energy theorems for the strong interaction w and z amplitudes. These theorems hold because in the absence of the gauge boson sector, w and z are by construction the Goldstone bosons of a spontaneously broken chiral $SU(2)$ symmetry. The low energy theorems are exact to all orders in the strong interactions. They can be derived by current algebra techniques or more conveniently from the effective Lagrangian of the sigma model, which reproduces the content of current algebra and $PCAC$.

In Section 3 we discuss this effective Lagrangian for a strongly interacting W_L, Z_L system, using w, z as interpolating fields. We present a variation on the standard

unitarily argument[2] which for asymptotically high energy, $s \gg m_H^2$, identifies the value, m_H, of the Higgs mass at which perturbation theory fails; our variation identifies the value of s at which perturbation theory fails for asymptotically large m_H, $m_H^2 \gg s$. We further explicate the chiral symmetry properties[10] of the effective Lagrangian and discuss "soft meson theorems" in the context of the minimal model. The results are equally applicable to all other models possessing a spontaneously broken global $SU(2)_L$ x $SU(2)_R$ symmetry, such as technicolor[4] and some ultracolor[5] models. The pervasiveness of models with such a spontaneously broken chiral $SU(2)$ is no accident, since it offers an elegant means of ensuring the existence of a "custodial" $SU(2)$ to protect the relation $\rho \equiv M_W^2/M_Z^2 cos^2\theta_W = 1$ to all orders in the strong w, z interactions.[11]

For such models the behavior of the strongly interacting W_L, Z_L system is uniquely specified for a "low" energy ($s \ll m_H^2, m_{Tc}^2$) region above ($s \gg M_{W,Z}^2$) the two body production threshold. This is precisely analogous to the region of validity, ($m_\pi^2 \ll s \ll m_{Hadron}^2$) of the soft pion theorems of hadronic physics. At what scale extrapolation of the low energy behavior breaks down, and what form scattering matrix elements take beyond that scale, would remain to be determined at the SSC. In particular, our results show that large WW, ZZ, and WZ production cross sections at the SSC could even signal the existence of new strong interaction sectors which are too heavy to be produced and studied directly at the SSC.

Section 4 contains our principal results for the study of new, TeV scale strong interactions at the hadron colliders proposed for the 1990's. If W_L and Z_L have strong interactions, we find that boson-boson fusion will provide an anomalous two gauge boson yield that can be observed at a collider with energy near 40 TeV and luminosity approaching $10^{33} cm.^{-2} sec.^{-1}$. In particular, we study two strong interaction models in some detail — the standard model with $m_H = 1\ TeV$ and a second model based on the low energy theorems discussed in Section 3. For these models we compute production cross sections for the six final states – ZZ, W^+Z, W^-Z, W^+W^-, W^+W^+, W^-W^- — assuming four pp collider center of mass energies, $\sqrt{s}$ = 10, 20, 30, 40 TeV. With appropriate cuts in rapidity and diboson invariant mass, we compare the results to the yields from $\overline{q}q$ annihilation. Finally we present some estimates of how the total event rates can be translated into event rates for experimentally reconstructable final states. Preliminary versions of some of these results have been presented in our earlier work[6] and in SSC workshops.[12,13]

In order to develop a feeling for the range of possibilities, we have also considered

in Section 4 three additional strong interaction models. Two, which are unitary models that obey the low energy theorems of Section 3, are for comparison with our principal model based on an extrapolation of the low energy theorems. The third, techni-rho production by diboson fusion in an $SU(N)_{TC}$ technicolor model with N = 2, 4, 6, is intended to explore the possible effect of resonances on the two gauge boson yield.

In Section 5 we briefly review previous results[6,12,13] for production of $n > 2$ bosons, including a new estimate of the four boson yield.

Section 6 is a brief summary and conclusion.

2.The Equivalence Theorem

In this Section we discuss in some detail the equivalence between S-matrix elements for external longitudinally polarized W_L, Z_L and those for the corresponding unphysical scalar particles, w, z. The reason for this is three-fold. First we wish to demonstrate explicitly that the result holds for $S-$matrix elements of w, z as calculated using the Feynman rules of the R_ξ gauge;[14] this has not been done in the previous literature[2,8,9] Secondly there are some subtleties involved in extracting the leading $0(m/E)$ behavior for multiparticle external states, for example the argument[2] of Lee et al. does not generalize in a straightforward way to the multiparticle case. Finally, we wish to study the validity of the equivalence theorem beyond the tree approximation; Cornwall et al.,[8] for example, claim only to have demonstrated equivalence at the tree level. While we are not interested in higher order corrections in the weak gauge couplings, our results are meaningful only if they are valid to all orders in the scalar self coupling $\lambda = m_H^2/2v^2$, since we are studying the strong coupling limit for that sector.

We first show that the Ward identity needed for the validity of the equivalence theorem is the one given in Eq. (2.1) below; we will then derive that identity to arbitrary order in perturbation theory.

The identity we need can be expressed as:

$$\begin{aligned} &\Delta(r,s,m) = 0 \qquad r \geq 1,\ s \geq 0, \\ &\Delta(r,s,m) = \sum_{M_i=0}^{4} \sum_{\mu_j=0}^{3} \Big(\prod_{i=1}^{r} m_{a_i}^{-1} D_{a_i}^{M_i}(p_i)\Big)\Big(\prod_{j=1}^{s} \epsilon_{(L)b_j}^{\mu_j}(q_j)\Big), \\ &\qquad \times S^{a_1\ldots a_r, b_1\ldots b_s}_{M_1\ldots M_r, \mu_1\ldots\mu_s A_1\ldots A_m}(p,q,k) \end{aligned} \tag{2.1}$$

which is a condition on the $S-$matrix elements for r vectors and/or unphysical scalars with momenta $p_1 \ldots p_r$, s longitudinally polarized vectors with momenta $q_i \ldots q_s$, and m other particles (fermions, physical Higgs particle, transversely polarized vectors) with all momenta on shell. The $A_\ell, \ell = 1 \ldots m$, denote the spin and internal quantum numbers of the last m particles, and $a, b = W^\pm, Z$. In writing (2.1) we have introduced a 5−component field $\tilde{V}_M^a = (V_\mu^a, \varphi^a)$, with φ^a the unphysical scalar eaten by the vector field V_μ^a, and a 5−component operator:

$$D_M^a(p) = (-ip_\mu, m^a) \tag{2.2}$$

such that if $\epsilon_a^\mu(p) S^{a\cdots}_{\mu\cdots}(p,\ldots)$ and $S^{a\cdots}_{4\cdots}(p,\cdots)$ are $S-$matrix elements with one external V^a and φ^a, respectively, of (out-going) momentum p, and all other external particles the same, then

$$\sum_{M=0}^{4} D_a^M(p)\ S^{a\cdots}_{M\cdots}(p,\ldots) \equiv -i \sum_{\mu=0}^{3} p^\mu\ S^{a\cdots}_{\mu\cdots}(p,\ldots) + m_a\ S^{a\cdots}_{4\cdots}(p,\ldots). \tag{2.3}$$

In the following we will usually drop explicit summations over the M_i and μ_j; it is to be understood that internal indices (a, b, A) are not summed except when explicitly indicated. We shall further compactify notation by writing, for example,

$$S[(a,M,p)_r\ (b,\mu,q)_s (A,k)_m] \equiv S^{a_1\ldots a_r, b_1\ldots b_s}_{M_1\ldots M_r, \mu_1\ldots\mu_s, A_1\ldots A_m}(p,q,k) \tag{2.4}$$

for the $S-$matrix element of Eq. (2.1).

To see that the identity (2.1) assures the equivalence theorem, we write the longitudinal polarization vector for a vector boson V^a of momentum p as:

$$\epsilon_{(L)\mu}^a\ (p)\ = p_\mu/m_a + v_\mu^a(p) \tag{2.5}$$

where $v_\mu^a(p)$ is a four-vector with components of order m_a/E for $E \gg m_a$. Since the vertex functions $S[(b,\mu,q)_n \cdots]$ that determine $S-$marix elements including n external vectors b_i of momentum q_i are at most logarithmically divergent for vanishing vector masses, $m_{b_i} \to 0$, we may write

$$\begin{aligned} V(\ell,n,m) &\equiv \Big(\prod_{i=1}^{r} v_{b_i}^{\mu_i}\Big)\ S[(a,4,p)_\ell\ (b,\mu,q)_n\ (A,k)_m] \\ &= 0[(m/E)^n] \end{aligned} \tag{2.6}$$

Defining:

$$\begin{aligned} X(\ell,r,s,m) \equiv &\Big(\prod_{i=1}^{r} m_{b_i}^{-1} q_i^{\mu_i}\Big)\Big(\prod_{j=i}^{s} \epsilon_{(L)c_j}^{\nu_j}(\kappa_j)\Big) \\ &\times S[(a,4,p)_\ell\ (b,\mu,q)_r\ (c,\nu,\kappa)_s\ (A,k)_m], \end{aligned} \tag{2.7}$$

summing $V(\ell,n,m)$ over all independent permutations among the (a_i,p_i) and (b_i,q_i), and using (2.5) to eliminate the $v_{b_i}^{\mu_i}$, we obtain the relation:

$$\overline{V}(\ell,n,m)=\sum_{s=0}^{n}(-)^{n-s}\,\overline{X}(\ell,n-s,s,m)=0[(m/E)^n], \tag{2.8}$$

where barred quantities imply a sum over all independent permutations of the $(a_i,p_i),(b_i,q_i)$ and (c_i,κ_i) that specify the momentum and electroweak charge of the unphysical scalars and longitudinally polarized vectors. Using the definition (2.2), the condition (2.1) may be written

$$\begin{aligned}\bar{\Delta}(r,s,m)&=\sum_{\ell=0}^{r}(-i)^{r-\ell}\,\bar{X}(\ell,r-\ell,s,m)=0\\&=\sum_{\ell=0}^{n-s}(-i)^{n-s-\ell}\,\bar{X}(\ell,n-s-\ell,s,m)\end{aligned} \tag{2.9}$$

where in the last term we have made the substitution $r=n-s$. Multiplying (2.9) by $(i)^s$ and summing over s, we obtain

$$\begin{aligned}\sum_{s=0}^{n-1}(i)^s\overline{\Delta}(n-s,s,m)&=0=\sum_{s=0}^{n-1}(-)^s\sum_{\ell=0}^{n-s}(-i)^{n-\ell}\,\overline{X}(\ell,n-s-\ell,s,m)\\&=\sum_{s=0}^{n}(-)^s\sum_{\ell=0}^{n-s}(-i)^{n-\ell}\,\bar{X}(\ell,n-s-\ell,s,m)-(i)^nX(0,0,n,m)\\&=\sum_{\ell=0}^{n}(i)^{n-\ell}\sum_{s=0}^{n-\ell}(-)^{n-\ell-s}\,\overline{X}(\ell,n-s-\ell,s,m)-(i)^nX(0,0,n,m)\\&=\sum_{\ell=0}^{n}(i)^{n-\ell}\,\overline{V}(\ell,n-\ell,m)-(i)^nX(0,0,n,m)\end{aligned} \tag{2.10}$$

where the last equality in (2.10) follows from Eq. (2.8). Since $\overline{V}(\ell,n-\ell,m)$ is of order $(m/E)^{n-\ell}$ we retain only the term with $n=l$ to obtain:

$$\overline{V}(n,0,m)=V(n,0,m)=(i)^nX(0,0,n,m)+0(m/E) \tag{2.11}$$

From the definitions (2.6) and (2.7), Eq. (2.11) reads:

$$\begin{aligned}S[(a,4,p)_n\,(A,k)_m]=(i)^n\,(\prod_{i=1}^{n}\epsilon^{\mu_i}_{(L)a_i})\,S[(a,\mu,p)_i(A,k)_m]\\+0(m/E).\end{aligned} \tag{2.12}$$

Eq. (2.12) is the statement that $S-$matrix elements for n longitudinally polarized vector bosons ($M_i=\mu_i$) and m other physical particles are the same, up to a phase and up to $0(m/E)$ corrections as the $S-$matrix elements obtained by replacing each longitudinally polarized vector boson by its corresponding unphysical scalar ($M_i=4$).

Notice that Eq. (2.5) does <u>not</u> imply, for example, that

$$\begin{aligned}\epsilon^{\mu_1}_{(L)a_1}(p_1)\epsilon^{\mu_2}_{(L)a_2}(p_2)S^{a_1a_2\cdots}_{\mu_1\mu_2\cdots}(p_1,p_2\cdots)=\frac{p_1^{\mu_1}}{m_1}\frac{p_2^{\mu_2}}{m_2}S^{a_1a_2\cdots}_{\mu_1\mu_2\cdots}(p_1,p_2\cdots)\\\times[1+0(m/E)].\end{aligned}$$

The reason is that, as is well known, gauge theory cancellations remove the leading $0[(p/m)^n]$ behavior for n external longitudinally polarized vectors. The non-leading contributions need not be correspondingly suppressed. For example, explicit calculations of the amplitudes for $q\bar{q}\to W_L^+W_L^-$ and $\gamma\gamma\to W_L^+W_L^-$ in the tree approximation show that

$$\epsilon^{\mu_1}_{(L)W}(p_1)\epsilon^{\mu_2}_{(L)W}(p_2)S^{W^+W^-}_{\mu_1\mu_2[q\bar{q}\ or\ \gamma\gamma]}-\frac{1}{M_W^2}p_1^{\mu_1}p_2^{\mu_2}S^{W^+W^-}_{\mu_1\mu_2[q\bar{q}\ or\ \gamma\gamma]}=0(1),$$

while

$$\epsilon^{\mu_1}_{(L)W}(p_1)\epsilon^{\mu_2}_{(L)W}(p_2)S^{W^+W^-}_{\mu_1\mu_2\,[q\bar{q}\ or\ \gamma\gamma]}+S^{W^+W^-}_{44\,[q\bar{q}\ or\ \gamma\gamma]}=0(m/E). \tag{2.13}$$

We have further verified (2.1) explicitly in tree level for $q\bar{q}\to W_L^+W_L^-$.

To derive the Ward identity (2.1), we introduce an auxiliary field B_a for each vector field ($a=W^\pm,Z,\gamma$), and write the gauge fixing term as

$$\mathcal{L}_{GF}=\sum_a\left(\frac{1}{2}B_a^2-\frac{1}{\sqrt{\xi_a}}B_aF_a\right),\quad F_a=\sum_M D^M_{Fa}\tilde{V}^a_M \tag{2.14}$$

where D^M_{Fa} is a 5−component derivative operator expressed in momentum space as

$$D^M_{Fa}(p)=(i\xi_ap^\mu,m_a) \tag{2.15}$$

where $m_a=0$ when "a" denotes the photon, $a=\gamma$. Using the equation of motion

$$0=\frac{\partial\mathcal{L}}{\partial B_a}=B_a-\frac{1}{\sqrt{\xi_a}}F_a, \tag{2.16}$$

one recovers the usual gauge fixing term in the R_ξ gauge[14]

$$\mathcal{L}_{GF} = -\frac{1}{2}\sum_a \xi_a^{-1} \mid F_a \mid^2. \tag{2.17}$$

We start with the result[15] that the renormalized generating functional $\Gamma(A)$ for one-particle irreducible Green's functions—where A represents all physical fields as well as unphysical scalars, Fadeev-Popov ghosts and the auxiliary fields B_a— is invariant under the improved BRS transformation[16]

$$0 = \sum_j \int d^4x \hat{\delta} A_j(x) \frac{\delta \Gamma(A)}{\delta A_j} \tag{2.18}$$

with (all repeated indices summed)

$$\hat{\delta} A_i = x^a_{ij} c_a A_j - \delta_i^{aM} \hat{D}_{aM} c_a + \delta_i^{\bar{c}_a} \sqrt{\xi}_a B_a, \tag{2.19}$$

where c_a and $\bar{c}_a$ are ghost and anti-ghost fields, respectively, $\chi^a_{ij} = 0(g)$ is the matrix element of the generator T^a between states * and $\hat{D}$ is a 5-component derivative operator defined in momentum space as

$$\hat{D}^M_a(p) = (ip^\mu, m_a) = D^M_a(-p) \tag{2.20}$$

The generating functional $W(J)$ for connected Green's functions is related to $\Gamma(A)$ by[17]

$$\begin{aligned} &W(J) + \Gamma(A) + \sum_i \int d^4x J_i(x) A_i(x) = 0 \\ &\frac{\delta W}{\delta J_i(x)} = -A_i(x) \quad , \quad \frac{\delta \Gamma}{\delta A_i(x)} = -J_i(x) \end{aligned} \tag{2.21}$$

In the following we will work in momentum space, where the transformation (2.19) is expressed as (all repeated indices summed):

*The matrices χ^a_{ij} are defined as follows: for ghosts $\chi_{\bar{c}_b i} = 0$, $\chi^d_{c_a c_b} = (\frac{1}{2}) g f_{abd}$, where $f_{abd}$is the structure constant; for $\chi^a_{(Mb),(Nd)}$ we define $\chi^a_{(4b),(\nu d)} = \chi^a_{(\mu b),(4d)} = 0, \chi^a_{(\mu b),(\nu d)} = g g_{\mu\nu} f_{abd}$, and $\chi^a_{(4b),(4d)} = g f_{abd}$; and we set $\chi_{B_b i}, = 0$ to ensure $\hat{\delta} B_a = 0$. We identify the physical Higgs field with the $M = 4$ component of the photon field, $a = \gamma$; it vanishes on contraction with D, $\hat{D}$, or D_F since $m_a = 0$ for $a = \gamma$.

$$\begin{aligned} \hat{\delta} A_i(k) = &\int \frac{d^4q}{(2\pi)^4} \chi^a_{ij} \, c_a(k-q) \, A_j(q) \; - \; \delta_i^{(aM)} \, D^a_M(-k) c_a(k) \\ &+ \delta_i^{\bar{c}_a} B_a(k) \sqrt{\xi}_a \end{aligned} \tag{2.22}$$

To obtain Ward identities for the connected Green's functions, we write $W(J)$ as an expansion in the J_i:

$$\begin{aligned} W(J) = &\sum_n \int (\prod_{i=1}^n \frac{d^4p_i}{(2\pi)^4}) (2\pi)^4 \, \delta^4(\sum p_i) J_{i_1}(-p_1) \cdots J_{i_n}(-p_n) \\ &\times W_{i_1 \cdots i_n}(p_1 \cdots p_n) \end{aligned} \tag{2.23}$$

Then

$$\begin{aligned} A_i(k) = -\frac{\delta W}{\delta J_i(-k)} = -\sum_n \int (\prod_{j=1}^n \frac{d^4p_j}{(2\pi)^4} \, J_{i_j}(-p_j)) \, W_{i \, i_1 \cdots i_n}(k, p_i \cdots p_n) \\ \times (2\pi)^4 \, \delta^4(k + \Sigma p_j) \end{aligned} \tag{2.24}$$

We now proceed to evaluate the identity

$$0 = \frac{\delta}{\delta J_{\bar{c}_b}(-k)} \prod_{j=1}^n (\frac{\delta}{\delta J_{i_j}(-p_j)}) \sum_i \int \frac{d^4q}{(2\pi)^4} \, J_i(-q) \, \hat{\delta} A_i(q) \Big|_{J=0}, \tag{2.25}$$

which follows from (2.18), using the definitions (2.22) and (2.24).

Let us first evaluate (2.25) for $n = 1$, $p_1 \equiv -p, i_1 = i_n \equiv i$. Substituting the expressions (2.24) for the field variables in the transformation (2.22), we see that the first term in (2.22), which is bilinear in fields, does not contribute to (2.25) for $n = 1$. * We then obtain a relation among propatators:

$$\sum_{a,M} \delta_i^{(Ma)} \, D^a_M(p) \, W_{c_a \bar{c}_b}(p) = \sqrt{\xi}_b W_{B_b i}(p). \tag{2.26}$$

*To verify this it is useful to know that the physical Higgs fields which can appear on the right side of Eqs. (2.19) and (2.22), $A^{a=\gamma}_{M=4}$, are shifted fields, with vanishing vacuum expectation values.

Taking $i = Ma$, the equation of motion (2.16) for B_a may be used to convert (2.26) into relations among ghost, vector and unphysical scalar propagators:

$$D_{Ma}(p)W_{c_a\bar{c}_b}(p) = \sum_N D^N_{Fb}(p)W_{Nb,Ma}(p), \tag{2.27}$$

that are readily verified for the tree approximation in the R_ξ gauge.

Next we evaluate (2.25) for $i_1 \cdots i_n = B_{a_1} \cdots B_{a_s}\ A_1 \cdots A_m$, where the A_i represent any physical particles including vector bosons with physical polarization ($\epsilon_\mu(p)p^\mu = 0$, $\epsilon = \epsilon_L$ or ϵ_T), with off-shell momenta $p_1 \cdots p_m$,and the B_{a_i} are auxiliary fields with off-shell momenta $k_1 \cdots k_s$. (The on-shell limit will be taken below.) The second term in the expression (2.19) for $\hat{\delta}A_i$ will contribute in this case only if one of the i_j denotes a vector boson ($\delta^{(a,\mu)}_{i_j} \neq 0$). However, for $i_j = (a,\mu)$, this term drops out upon contraction with a physical polarization vector, $\epsilon^\mu_a(p_j)D^a_\mu(p_j) = 0$, so it does not contribute to the case considered here. When substituted into (2.25), the first term in (2.22) gives rise to terms of the form:

$$\sum_a \chi^a_{A_1A'_1}\, W_{c_a\bar{c}_bB_{a_1}\ldots B_{a_r}A_2\ldots A_t}(p_1 - q, k, k_1 \ldots k_r, p_2 \ldots p_t) \times W_{A'_1B_{a_{r+1}}\ldots B_{a_s}A_{t+1}\ldots A_m}(q, k_{r+1} \ldots k_s, p_{t+1} \ldots p_m) \tag{2.28}$$

where

$$q = -\sum_{i=r+1}^{s} k_i - \sum_{i=t+1}^{m} p_i$$

and

$$k = -\sum_{i=1}^{s} k_i - \sum_{i=1}^{m} p_i$$

are off-shell momenta. The off-shell $S-$matrix elements $\tilde{S}$ are related to the connected Green's functions W by products of external propagators W_{ij}:

$$W_{i_1\ldots i_n}(p_1 \cdots p_n) = (\prod_{\ell=1}^{n} W_{i_\ell i'_\ell}(p_\ell))\tilde{S}_{i'_1\ldots i'_n}(p_1 \cdots p_n) \tag{2.29}$$

If we multiply (2.25) by the product of inverse propagators for each physical field A_i, and set the A_i on mass shell, each term of the type (2.28) vanishes because there is always one off-shell momentum giving rise to a factor of the form:

$$W^{-1}_{A_1A_1}(p_1)W_{A'_1A'_1}(q) \overset{p_1^2=m_1^2}{\longrightarrow} 0.$$

Thus we need only consider the contribution of the last term in (2.22), which when inserted in (2.25) takes the form:

$$\begin{aligned} 0 &= \sqrt{\xi_b}W_{B_bB_{a_1}\ldots B_{a_s}A_1\ldots A_m}(k, k_i, p_i) \\ &= \sqrt{\xi_b}(\prod_{i=1}^{m} W_{A_iA_i}(p_i))\sum_{\ell,\ell_j}(\prod_{j=1}^{s} W_{B_{a_j}\ell_j}(k_j))W_{B_b l}(k) \times \tilde{S}_{\ell\ell_1\ldots\ell_sA_1\ldots A_m}(k, k_i, p_i) \\ &= \sum_{d_j,M_j}(\prod_{i=1}^{m} W_{A_iA_i}(p_i))(\sum_{j=1}^{s} \xi^{-1/2}_{a_j}W_{c_{d_j}\bar{c}_{a_j}}(k_j)D^{M_j}_{d_j}(k_j))W_{c_{d_{s+1}}\bar{c}_b}(k)D^{M_{s+1}}_{d_{s+1}}(k) \\ &\times \tilde{S}[(d, M, k)_{s+1}(A, p)_m] \end{aligned} \tag{2.30}$$

where $\tilde{S}$ has been expressed in the notation of Eq. (2.4) with $k \equiv k_{s+1}$. In writing the last equality in (2.30) we used the relation (2.27) for two point functions. Multiplying (2.30) by the inverse propagators for the physical fields A_i and for the ghost-fields and also by the factor

$$\prod_{j=1}^{s} \xi^{1/2}_{a_j},$$

and setting the A_i on mass-shell, we obtain from the above argument the desired Ward Identity:

$$\sum_{M_j}(\prod_{j=1}^{s+1} D^{M_j}_{d_j}(k_j))\tilde{S}[(d, M, k)_{s+1}(A, p)_m]\Big|_{p_i^2=m_i^2} = 0. \tag{2.31}$$

Equation (2.31) is valid to arbitrary order in perturbation theory and for off-shell values of the k_i. Putting the k_i on shell, $k_i^2 = m^2_{d_i}$, we recover the Ward identity (2.1) for physical $S-$matrix elements: $S(p_i) = \tilde{S}(p_i)|_{p_i{}^2=m_i^2}$, where in 2.31, some number $r \leq m$ of the fields A_i can be taken as longitudinally polarized vector bosons.

The Ward identity (2.31) may also be derived without the use of the auxiliary fields B_a. In this case the last term in (2.19) is replaced by $\delta^{c_a}_i D^M_{Fa}\tilde{V}^a_M$ and the Ward identity is obtained by evaluating (2.25) for $i_j = (aM)_1, \cdots (aM)_s, A_1 \cdots A_m$. Then additional terms, arising from both the first and second terms of (2.19), appear on

the right hand side of (2.31); these are eliminated by using the equations of motion for the antighost field:

$$0 = \frac{\partial \mathcal{L}_{Ghost}}{\partial \bar{c}_a} = \sum_M D^M_{Fa}\, \hat{\partial}\, \tilde{V}^a_M$$

$$\mathcal{L}_{Ghost} = \sum_{\text{all indices}} \frac{1}{\xi_a} \bar{c}_a D^{aM}_F [(\chi^b_{aM,dN} \tilde{V}^N_d - \hat{D}^a_M) c_b] \qquad (2.32)$$

$$= \sum_{a,M} \bar{c}_a D^M_{Fa} \hat{\partial} \tilde{V}^a_M$$

Having established the equivalence theorem (2.12), we turn in the next section to a discussion of the properties of the unphysical scalars that may be ascribed, to $0(m/E)$, to the longitudinally polarized vectors.

3. The Effective High Energy Theory

Exploiting the results of the preceeding section, we consider the Lagrangian of the minimal electroweak model in the R_ξ gauge:

$$\mathcal{L} = \mathcal{L}_g - V \qquad (3.1)$$

where $\mathcal{L}_g$ includes the covariant kinetic energy terms (Yang-Mills and gauge couplings), gauge fixing and gauge compensating (ghost) terms, masses and Yukawa couplings. For the purposes of this paper we assume that the Yukwawa couplings are weak ($G_{yuk} \leq 0(g)$), in other words that there are no fermions considerably more massive than the W that acquire their mass through couplings to the standard Higgs doublet. The case of a strongly interacting Yukawa sector is of interest in itself[18] and could provide an additional source of multiple Higgs and/or W, Z production,[19] but here we disregard that possibility.

The Higgs potential V in (3.1) is given by

$$V = \frac{m_H^2}{2} H^2 + \frac{1}{2}\frac{m_H^2}{v}(\vec{\varphi}^2 + H^2) H + \frac{m_H^2}{8v^2}(\vec{\varphi}^2 + H^2)^2 \qquad (3.2)$$

where H is the physical Higgs scalar, $v = (\sqrt{2}G_F)^{-1/2}$ is the vacuum expectation value of the unshifted scalar field, and

$$\vec{\varphi} \equiv (w_1, w_2, z) \equiv (\varphi_1, \varphi_2, \varphi_3), \quad w_\pm = \frac{1}{\sqrt{2}}(w_1 \mp i w_2) \qquad (3.3)$$

are the unphysical scalars whose $S-$matrix elements satisfy the identities (2.1), (2.13) and (2.31) of the previous section:

$$w^\pm \equiv \varphi_{W\pm}, \; z \equiv \varphi_Z. \qquad (3.4)$$

The usual complex Higgs doublet Φ that transforms as

$$\delta\Phi = \frac{g}{2} i\vec{\lambda} \cdot \vec{\tau} \Phi \qquad (3.5)$$

under the infinitesimal $SU(2)$ gauge transformation

$$\delta W_i = \partial \lambda_i - g \epsilon_{ijk} \lambda^j W_k \qquad (3.6)$$

is expressed in terms of the φ_i as

$$\Phi = \begin{pmatrix} -iw^+ \\ [\frac{1}{\sqrt{2}}(H+v-iz)] \end{pmatrix}. \tag{3.7}$$

As is well known,[1] since the vev is fixed by experiment, the quartic ($\lambda = m_H^2/2v^2$) and cubic ($m_H^2/2v$) scalar self-couplings become strong as the Higgs mass approaches one TeV. In this limit we must work to all orders in the potential V. We shall therefore consider the scalar sector as a strongly interacting system in the presence of weakly coupled external sources, namely the gauge and Yukawa couplings that we treat in lowest non-trivial order. We do not propose to solve(!) the dynamics of the strongly coupled scalar sector, but rather to exploit its symmetries and the analogue of $PCAC$ to make some statements about $S-$matrix elements for external w's and z's. The equivalence theorem then allows us to translate these into approximate statements on matrix elements for longitudinally polarized W's and Z's.

The potential V is invariant under parity with H defined as a scalar and the φ_i as pseudoscalars. It is further invariant under a global vector $SU(2)$, with infinitesimal transformations:

$$\delta_j^V \varphi_i = \kappa_V \epsilon_{jik}\varphi_k, \quad \delta_j^V H = 0, \tag{3.8}$$

and a global, nonhomogeneous "axial" $SU(2)$:

$$\delta_i^A H = -\kappa_A \varphi_i, \quad \delta_i^A \varphi_j = \delta_{ij}\kappa_A(H+v) \tag{3.9}$$

($\kappa_{V,A}$ are the infintesimal parameters of the transformations) that together form a Goldstone-realized "chiral" $SU(2)$ x $SU(2)$ invariance group. The conserved currents, obtained from the full scalar Lagrangian

$$\mathcal{L}_\varphi = \frac{1}{2}(\partial_\mu \varphi)^2 + \frac{1}{2}(\partial_\mu H)^2 - V \tag{3.10}$$

are given by

$$\begin{aligned} V_\mu^i &= \kappa_V^{-1}\frac{\partial \mathcal{L}_\varphi}{\partial(\partial_\mu \varphi_i)}\delta_i^V \varphi^j = \varepsilon_{ijk}(\partial_\mu \varphi_j)\varphi_k, \\ A_\mu^i &= \kappa_A^{-1}[\frac{\partial \mathcal{L}_\varphi}{\partial(\partial_\mu \varphi_j)}\delta_i^A \varphi_j + \frac{\partial \mathcal{L}_\varphi}{\partial(\partial_\mu \mathrm{H})}\delta_i^A H] \\ &= -(\partial_\mu H)\varphi_i + (\partial_\mu \varphi_j)(H+v). \end{aligned} \tag{3.11}$$

It is easy to check, using the equations of motion for the fields φ_i and H, that the vector and axial currents are conserved:

$$\partial^\mu V_\mu = \partial^\mu A_\mu = 0 \tag{3.12}$$

and that they satisfy the usual $SU(2)$ x $SU(2)$ current algebra:

$$\begin{aligned} [Q_i, V_\mu^j] = [Q_i^5, A_\mu^j] &= i\varepsilon_{ijk}V_\mu^k \\ [Q_i, A_\mu^j] = [Q_i^5, V_\mu^J] &= i\varepsilon_{ijk}A_\mu^k, \end{aligned} \tag{3.13}$$

where

$$Q_i = \int d^3x V_o^i(x) \tag{3.14}$$

and

$$Q_i^5 = \int d^3x A_o^i(x) \tag{3.15}$$

are the generators of the transformations (3.8) and (3.9), respectively.

It is clear that Weinberg's analysis[20] of low energy $\pi - \pi$ scattering amplitudes in the exact chiral limit, $m_\pi \to 0$, can be transcribed verbatim to the description of w, z scattering amplitudes if $\mathcal{L}_g$ is neglected. For $m_H^2 \gg \hat{s}$, the result will simply reproduce the tree approximation as calculated using the Lagrangian (3.10), since by construction the latter satisfies the constraints of chiral symmetry. This assertion can be made more transparent if one redefines the fields by a transformation

$$\Phi = e^{i\frac{\vec{t}\cdot\vec{\delta}}{v}}\begin{pmatrix} 0 \\ \frac{H'+v}{\sqrt{2}} \end{pmatrix} \tag{3.16}$$

that removes the scalars from the potential V, as in defining the unitary gauge. In the Lagrangian (3.10) they reappear with derivative couplings through the kinetic

energy term. The Lagrangian obtained in this way is to be interpreted as an effective Lagrangian for tree amplitudes that automatically satisfy the chiral symmetry constraints; in particular the derivative couplings assure Goldstone decoupling at zero energy. Since a field redefinition does not change $S-$matrix elements, the tree approximation to the linear $\sigma-$model, Eq. (3.10), gives the same amplitudes as the tree approximation to the non-linear σ-model obtained with the transformation (3.16). The non-linear formulation (using a slightly different field redefinition) has been studied previously in various contexts.[10]

The tree amplitudes for w and z scattering have been given in Ref. 2; they are:

$$T(w^+w^- \to w^+w^-) = -\sqrt{2}G_F m_H^2\left(\frac{s}{s-m_H^2}+\frac{t}{t-m_H^2}\right) \tag{3.17a}$$

$$T(zz \to zz) = -\sqrt{2}G_F m_H^2\left(\frac{s}{s-m_H^2}+\frac{t}{t-m_H^2}+\frac{u}{u-m_H^2}\right) \tag{3.17b}$$

$$T(w^+w^- \leftrightarrow zz) = -\sqrt{2}G_F m_H^2\frac{s}{s-m_H^2}. \tag{3.17c}$$

Note that the charge exchange process $w^+w^- \leftrightarrow zz$ occurs only in the $s-$wave channel. Lee et al.[2] diagonalized the $S-$matrix for this system in the limit $s \gg m_H^2$, and found that the highest $s-$channel eigenvalue saturates tree unitarity if $m_H = 1\ TeV$. If we consider instead the limit $m_H^2 \gg s$, the same analysis shows that $s-$wave tree unitarity is saturated for $\sqrt{s} = 1.8\ TeV$. This means that for $m_H \gg 1\ TeV$, the tree approximation will cease to be valid beyond $2\ TeV$, if not sooner. On the other hand, chiral symmetry implies that the tree approximation is valid for some region above threshold. The tree amplitudes scale as s/v^2, and we expect them to be approximately accurate until some new scale parameter (e.g. the Higgs mass) becomes relevant and provides the appropriate damping. This scale will correspond to new, observable phenomena, which may or may not include an s-channel $I = 0$ resonance.

As an example consider the $O(2N)$ sigma model. In the large N limit the scattering amplitudes are unitarized at the scale $\sim\ 32\pi^2v^2/N$.[21] For a rough comparison with hadronic physics in the light quark sector (u and d only) we consider $N = 2$, since the $O(4)$ sigma model is precisely the $SU(2)_L$ x $SU(2)_R$ model of light quark phenomenology. Then with $v = F_\pi$ the unitarization scale is $\sim 1.2GeV$, which is of the order or larger than the scale of the bound state spectrum of nonstrange

quarks. Pursuing the analogy with hadronic physics, it is also amusing that the $I = J = 0$ scattering amplitude obtained[13] by scaling $\pi\pi$ data by v/F_π has a phase shift passing through 90^o at $\sqrt{s} \cong 2TeV$.

Let us now consider the scalar sector in the presence of gauge and Yukawa interactions. That part of the Lagrangian (3.1) that involves scalar fields can be decomposed as

$$\mathcal{L}(\varphi) = \mathcal{L}_\varphi + \mathcal{L}_{V\varphi^2} + \mathcal{L}_{V^2\varphi^2} + \mathcal{L}_{G.F.} + \mathcal{L}_{Ghost} + \mathcal{L}_{yuk} \tag{3.18}$$

where $\mathcal{L}_\varphi$ is defined in (3.10). $\mathcal{L}_{V\varphi^2}$ contains the gauge couplings to scalars that are linear in the gauge fields:

$$\begin{aligned}\mathcal{L}_{V\varphi^2} &= -i\Phi^\dagger \overleftrightarrow{\partial}\left(\frac{g}{2}\vec{\tau}\cdot W + g'B\right)\Phi \\ &= eA^\mu_{(\gamma)}V^3_\mu + \frac{g}{2\sqrt{2}}[W^{+\mu}(V^-_\mu + A^-_\mu) + h.c] \\ &+ \frac{g}{2cos\theta}Z^\mu\{A^3_\mu + V^3_\mu(1-2cos^2\theta)\},\end{aligned} \tag{3.19}$$

where $A^-_\mu = A^1_\mu + iA^2_\mu$ and $V^-_\mu = V^1_\mu + iV^2_\mu$ are defined as charge raising operators, and A_i and V_i are the conserved Noether currents (3.11). $\mathcal{L}_{G.F.}$ is the gauge fixing term, Eq. (2.17), and contains a pseudoscalar mass term

$$m^2_{\varphi_\alpha} = m^2_{V\alpha}/\xi_\alpha \tag{3.20}$$

where φ_α is the gauge parameter.

Let us first work in the "Landau" gauge defined here as the $\xi \to \infty$ limit of the R_ξ gauge. In this case the pseudoscalars remain massless and decouple from the ghosts (see Eq. (2.32)), and the gauge fixing term (2.17) becomes:

$$\lim_{\xi\to\infty}\mathcal{L}_{G.F.} = -\lim_{\xi\to\infty}\frac{\xi_\alpha}{2}|\partial^\mu V^\alpha_\mu|^2 + (\partial^\mu V^\alpha_\mu)\phi_\alpha. \tag{3.21}$$

Since the limit $\xi \to \infty$ imposes $\partial^\mu V^\alpha_\mu \equiv 0$, we may neglect the second term in (3.21). In other words the $V \leftrightarrow \varphi$ transition amplitude vanishes upon contraction with a physical external polarization vector $\epsilon \cdot p = 0$, or an internal propagator:

$$\partial^\mu \Delta_{\mu\nu}(x)_{\xi\to\infty} = 0. \tag{3.22}$$

Thus in the "Landau gauge", the scalar sector is exactly chiral $SU(2)$ invariant, with the chiral invariance broken only by the weak Yukawa and gauge couplings. The Yukawa couplings of scalar (H) and pseudoscalar (φ_i) densities have well defined transformation properties, Eq. (3.8) and (3.9), under chiral $SU(2)$. The gauge bosons are coupled to the conserved vector and axial currents, Eq.(3.19). The situation is entirely anlogous to the chiral symmetric hadronic sector (in the limit $m_\pi \to 0$) of QCD in the presence of low energy weak interactions, and the same low energy theorems apply * to matrix elements of current and scalar densities between states of strongly interacting particles – in this case w and z. It is easy to check that, as expected, the tree approximation to the Lagrangian (3.1), (3.18) satisfies the current algebra constraints for amplitudes involving external w, z, and external sources, as well as for the purely strong w, z scattering amplitudes discussed above.

How does renormalization affect these results? First we note that the Landau gauge condition is not renormalized, and the poles in the unphysical scalar propagators are not shifted away from the origin. We interpret g, g' and the vector boson masses as their renormalized on-shell values; since we are working to lowest nontrival order in these quantities, the corresponding counter terms play no role. Finally, we define v as the renormalized coupling of the pseudoscalar field to the axial current,

$$< 0 \mid A^i_\mu \mid \varphi^j >\equiv i\delta_{ij} p_\mu v, \tag{3.23}$$

as measured by the muon lifetime:

$$v \equiv (\sqrt{2}G_F)^{-1/2}[1 + 0(g^2)] \tag{3.24}$$

up to $0(g^2)$ corrections that we are neglecting. To see that (3.23) and (3.24) are equivalent definitions,[10] we note that the scalar contribution to the $W^\pm$ self-energy is, from Eq. (3.19)

$$\Sigma^\varphi_{\mu\nu}(p) = \frac{g^2}{8}\int d^4x e^{-ipx}[< T(A^+_\mu(x), A^-_\nu(0) + V^+_\mu(x), V^-_\nu(0)) >]. \tag{3.25}$$

*For more than one external vector or axial current, the quartic gauge scalar couplings ($L_{V^2\varphi^2}$) cancel Schwinger terms so as to insure the naive current algebra manipulatons with the matrix elements of time ordered products replaced by T^* products.[22]

Current conservation (3.12), and Lorentz invariance of the vacuum $< V_\mu(0) >= 0$, imply that $\sum^\varphi_{\mu\nu}$ is divergenceless:

$$p^\mu \Sigma^\varphi_{\mu\nu}(p) = 0;\ \Sigma^\varphi_{\mu\nu}(p) \equiv \Sigma(p)(-g_{\mu\nu} + \frac{p_\mu p_\nu}{p^2}). \tag{3.26}$$

Now $\sum^\varphi_{\mu\nu}$ has a pole at $p^2 = 0$ arising from w-exchange (Fig.3a) with residue

$$\begin{aligned} p^2\Sigma_{\mu\nu}(p^2)\mid_{p^2=0} &= \frac{g^2}{8} < 0 \mid A^+_\mu \mid w^+ >< w^+ \mid A^-_\nu \mid 0 > \\ &= p_\mu p_\nu v^2 \frac{g^2}{4} \end{aligned} \tag{3.27}$$

where the last equality follows from the definition (3.23). Then for small p^2,

$$\Sigma_{\mu\nu}(p^2 \simeq 0) = \frac{g^2}{4}v^2(-g_{\mu\nu} + \frac{p_\mu p_\nu}{p^2}),$$

and the pole in the W-propagator is shifted according to

$$\begin{aligned} (\Delta_0)_{\mu\nu} \equiv \frac{1}{p^2}\left(-g_{\mu\nu} + \frac{p_\mu p_\nu}{p^2}\right) \to \Delta_{\mu\nu} &= \{\Delta_0 \sum_{n=0}^{\infty}(\Delta\Sigma)^n\}_{\mu\nu} \\ &= \left(-g_{\mu\nu} + \frac{p_\mu p_\nu}{p^2}\right)\left(p^2 - g^2v^2/4\right)^{-1} \end{aligned} \tag{3.28}$$

Corrections to this result from, for example, the diagrams in Fig. 3b are $O(g^2)$. The physical mass of the W is identified as the position of the pole in the propagator:

$$m^2_W = (g^2v^2/4)(1 + 0(g^2)),$$

which is equivalent to (3.24).

If we work instead in a gauge with finite ξ, the w, z acquire small masses:

$$m^2_i = m^2_{V_i}/\xi_i \tag{3.29}$$

and as a consequence the currents (3.11) are only partially conserved:

$$\begin{aligned} \partial^\mu A^i_\mu &= \frac{m^2_i}{\xi_i}\varphi_i v \\ \partial^\mu V^i_\mu &= \epsilon_{ijk} w_j w_k m^2_j/\,\xi_j \ \ (= 0\ if\ \xi_w = \xi_z). \end{aligned} \tag{3.30}$$

In this case current algebra must be implemented with the assumption that matrix elements of the axial current divergence are pseudoscalar pole dominated, and, as for finite pion masses in chiral pion dynamics, the same results are obtained to lowest order in m_i^2. It is worth noting that the explicit chiral symmetry breaking parameter m_i^2 and the spontaneous chiral symmetry breaking parameter v^2 are here in the ratio

$$(m_W/v)^2 = 0.11, \tag{3.31}$$

while the analogous parameters in the pion case are in the ratio

$$(m_\pi/f_\pi)^2 = 2.27,$$

so that the effects of explicit breaking are less important for the system studied here.* It follows, moreover, from the results of Section 2, that pseudoscalar amplitudes calculated in any R_ξ gauge can differ only in order m/E, since they differ only in that order from the ξ-independent physical amplitudes for longitudinally polarized vector mesons.

What we have done in this section is to display explicitly the chiral properties of the scalar sector in the R_ξ Lagrangian of the minimal electroweak model. The same properties hold a fortiori for the unphysical scalars of technicolor models, where they are by construction the Goldstone bosons of a spontaneously broken chiral symmetry. Such a chiral $SU(2)$ is a feature of a large class of experimentally viable models since conservation of the diagonal subgroup of $SU(2)_L$ x $SU(2)_R$ protects $\rho = (M_W/M_Z cos\theta_w)^2 = 1 + 0(\alpha)$ from strong interaction corrections.

Together with the results of Section 2, that again are expected to hold in more general models, the chiral properties discussed in this section permit us to determine, independently of perturbation theory, the couplings of longitudinally polarized vector mesons to one another and to weak external sources over some energy range $s_{threshold} \leq s \leq \Lambda^2$, where Λ is a scale parameter characterizing the strongly interacting system. The remaining sections of this paper will be devoted to the phenomenology of strongly interacting W's and Z's.

*However, there need be no simple relationship between symmetry breaking effects from $m_\pi \neq 0$ in the usual sigma model and symmetry breaking due to gauge interactions, since the latter include symmetry breaking terms that have no counterpart in the ungauged model with explicit pion mass $m_\pi \neq 0$.

4. Strong Interaction Signals in Two Body Channels

Two boson bremstrahlung,[7,6] shown in Figure 1, provides us with a beautiful probe of strong interactions among the W and Z bosons. Since kinematics requires that the bosons are emitted off the mass shell they must rescatter in order to appear in the final state. In the standard model with a light Higgs boson, the rescattering amplitude is weak, $O(\alpha)$, and Figure (1) is a negligible source of gauge boson pairs relative to $\bar{q}q$ annihilation shown in Figure 2. But when the rescattering amplitude is strong, Figures (1) and (2) are of the same order in α. In this case, for a sufficiently energetic hadron collider ($\sqrt{s} \geq O(40\ TeV)$, as we show below), there is a set of cuts such that the bremstrahlung mechanism is dominant. Measurement of the diboson yield satisfying these cuts (which are on the rapidity and diboson mass) is then a powerful test for the existence of new strong interactions.

4.1 Gauge boson luminosity distributions.

We will briefly sketch the derivation[23] of the longitudinal boson luminosity distributions obtained from Figure (1), for the sake of completeness and in order to explain a subtle and amusing feature. As emphasized above, it is only the longitudinal bosons which can have strong interactions, but they have negligible couplings $O(gm_q/M_W) + O(M_W/\sqrt{s})$, to the light quarks in Figure (1). How then can bremstrahlung be an important source of strongly interacting gauge bosons?

Our derivation proceeds by first computing the cross section to produce the Higgs boson by diboson fusion as shown in Figure (4). The cross section is (for $m_q = 0$)

$$\sigma = \frac{g^6 M_W^2 s}{64}\Big(\int_{LIPS}\Big) z_1 z_2 \frac{3 + 3c_1c_2 + c_1 + c_2 - 2s_1s_2\cos(\varphi_1 - \varphi_2)}{(q_1^2 - M_W^2)^2(q_2^2 - M_W^2)^2} \tag{4.1}$$

where LIPS stands for Lorentz Invariant Phase Space, s corresponds to the initial qq pair, $c_i = \cos\theta_i$ and $s_i = \sin\theta_i$ refer to the polar scattering angles of the quarks q_i, φ_i are their azimuthal angles, $z_i = 2E_i'/\sqrt{s}$ denotes the energy fraction retained by final state quark q_i', and the domain of integration is

$$\Big(\int_{LIPS}\Big) \equiv \int \frac{d^3p_H\, d^3p_1'\, d^3p_2'}{(2\pi)^9 8E_H E_1' E_2'}(2\pi)^4\delta(p_1 + p_2 - p_H - p_1' - p_2').$$

The integral is dominated by forward scattering angles, $\theta_i \cong 0$, which minimize the W propagators in the denominator. In the spirit of the Weizsacker-Williams

approximation for the analogous two photon process, we put $\theta_1 = \theta_2 = 0$ except in the propagators (where $\theta_i = 0$ would lead to a spurious singularity). In this approximation the cross section becomes

$$\sigma = \frac{g^6 M_W^2}{4(2\pi)^3 s^2} \int \frac{dz_1 dz_2 dc_1 dc_2}{z_H} \frac{\delta(2 - z_1 - z_2 - z_H)}{(1 - c_1 + 2M_W^2/z_1 s)^2 (1 - c_2 + 2M_W^2/z_2 s)^2} \tag{4.2}$$

with

$$z_H \cong \sqrt{\frac{4m_H^2}{s} + (z_1 - z_2)^2}$$

With the additional approximation $M_W^2 \ll s z_i$, the angular integrations yield factors

$$\int_{-1}^{1} \frac{dc_i}{(1 - c_i + 2M_W^2/z_i s)^2} \cong \frac{s z_i}{2M_W^2} \tag{4.3}$$

The rest of the integral can be done exactly, with the final result

$$\sigma = \frac{\alpha_w^3}{8M_W^2}\{-\frac{1}{2}(1+x)\ln x - (1-x)\} \tag{4.4}$$

where $\alpha_w \equiv \alpha/\sin^2\theta_w$ and $x \equiv m_H^2/s$.

It is only the longitudinally polarized W bosons which contribute to this result. Neglecting the quark mass, as we have, a transversely polarized boson cannot be emitted in the forward direction, so our small angle approximation has eliminated the contribution of the transverse components. Longitudinal bosons can be radiated in the forward direction, with the result shown in Eq. (4.3) that the angular integrations yield factors s/M_W^2. This factor is the key to understanding why the longitudinal components are able to contribute even in the limit of vanishing quark mass. The longitudinal wave function is

$$\varepsilon_L^\mu = \frac{1}{M_W}(p, O, O, E)$$

where $p^\mu = (E, 0, 0, p)$ is the four-momentum and $E^2 = p^2 + M_W^2$. For $E \gg M_W$,

$$\varepsilon_L^\mu \cong \frac{p^\mu}{M_W} - \frac{M_W}{2E}(1, 0, 0, -1)$$

The first term is the source of the common wisdom that the longitudinal component cannot couple to massless quarks. But the second term contributes a factor M_W^2/s to σ that is independent of the quark mass, which can contribute even as $M_W^2/s \to 0$ because it is just canceled by the factor s/M_W^2 from Eq. (4.3). (If we had kept terms of order θ_i, then the angular integrations would have yielded logarithmic factors from the transverse components, precisely as in the Weizsacker-Williams treatment of $\gamma\gamma$ scattering.)

The effective luminosity to find incident W^+W^- beams in parent beams of quarks and/or antiquarks can be obtained from Eq. (4.4) by unfolding the definition

$$\sigma(qq \to qqWW \to qqH) = \int dx \left.\frac{d\mathcal{L}}{dx}\right|_{WW/qq} \cdot \sigma(WW \to H) \tag{4.5}$$

Generalizing to all gauge boson types, $V_1V_2 = WW, WZ, ZZ$, the result is

$$\left.\frac{d\mathcal{L}}{dz}\right|_{V_1V_2/qq} = \frac{\alpha_w^2 \chi_1 \chi_2}{\pi^2}\frac{1}{z}[(1+z)\ln\frac{1}{z} - 2 + 2z] \tag{4.6}$$

where $\alpha_w = \alpha/\sin^2\theta_w, z = s_{VV}/s_{qq}$

and the χ_i are defined by

$$\begin{aligned} \chi_{Wu\bar{d}} &= \frac{1}{4} \\ \chi_{Zu\bar{u}} &= \frac{1 + (1 - \frac{8}{3}\sin^2\theta_w)^2}{16\cos^2\theta_w} \\ \chi_{Zd\bar{d}} &= \frac{1 + (1 - \frac{4}{3}\sin^2\theta_w)^2}{16\cos^2\theta_w}. \end{aligned} \tag{4.7}$$

Equation (4.6) gives the total yield of gauge boson pairs at a given z. In order to implement the rapidity cuts we will need to unfold Eq. (4.6),

$$\left.\frac{d\mathcal{L}}{dz}\right|_{V_1V_2/q_1q_2} = \int_z^1 du \left.\frac{d^2\mathcal{L}}{dzdu}\right|_{V_1V_2/q_1q_2} \tag{4.7a}$$

where

$$\left.\frac{d^2\mathcal{L}}{dzdu}\right|_{V_1V_2/q_1q_2} = \frac{\alpha_w^2 \chi_1 \chi_2}{\pi^2}\frac{(1-u)(u-z)}{zu^2} \tag{4.8}$$

and in the notation of Eq. (4.1) u is defined as $u = 1 - z_1$. The rapidity of the V_1V_2 center of mass system with respect to the q_1q_2 center of mass is then

$$y_q = \ln \frac{u}{\sqrt{z}}. \tag{4.9}$$

4.2 Calculation of Boson Pair Cross Sections.

The cross section to produce a pair of longitudinal gauge bosons by the double bremstrahlung mechanism is given by the gauge boson $2 \to 2$ scattering cross sections $d\sigma/d\cos\theta(V_1V_2 \to V_1'V_2')$ (θ being the VV center of mass scattering angle), convoluted with the luminosity distribution function $d\mathcal{L}/dz\,|_{V_1V_2/q_1q_2}$ to find V_1V_2 in the q_1q_2 beams, convoluted in turn with the quark luminosity $d\mathcal{L}/d\tau\,|_{q_1q_2/pp}$ to find the quarks in the incident proton beams. The quark luminosity distribution is

$$\left.\frac{d\mathcal{L}}{d\tau}\right|_{q_1q_2/pp} = \int_\tau^1 \frac{dx}{x} f_1(x) f_2(\frac{\tau}{x}) \tag{4.10}$$

where the f_i are the familiar probability functions, normalized, for example, so that

$$\int_0^1 dx(u(x) - \bar{u}(x)) = 2.$$

To implement the rapidity cut, we must unfold the x integration in Eq. (4.10), the u integration in (4.7), and the integration over $\cos\theta$, the V_1V_2 center of mass scattering angle. The result is a five dimensional integral, which in the absence of rapidity cuts would be

$$\sigma(pp \to V_1'V_2' + \cdots) = \int_{\tau_0}^1 d\tau_0 \sum_{\substack{q_1 \\ V_1}} \sum_{\substack{q_2 \\ V_2}} \{\int_\tau^1 \frac{dx}{x} f_1(x) f_2(\frac{\tau}{x}) \times \int_{\tau_0/\tau}^1 dz \int_z^1 du \left.\frac{d^2\mathcal{L}}{dzdu}\right|_{V_1V_2/q_1q_2} \cdot \int_{-1}^1 d\cos\theta \frac{d\sigma}{d\cos\theta}(V_1V_2 \to V_1'V_2')\} \tag{4.11}$$

To impose the rapidity cut on both final state bosons V_i' we must also restrict the domain of integration with the constraint

$$| y_P + y_q \pm y_V | \leq y_{MAX}. \tag{4.12}$$

Here y_V is the rapidity of V_1' in the VV center of mass (and $-y_V$ is that of V_2'),

$$y_V = \frac{1}{2}\ln(\frac{E + p\cos\theta}{E - p\cos\theta})_{c.m.s.} \tag{4.13}$$

where E and p are the c.m.s. energy and three-momentum of V_1'. (In computing y_V we use $M_W = 83GeV$ for both the W and Z masses.) The V_1V_2 rapidity with respect to the q_1q_2 c.m.s. is,

$$y_q = \ln \frac{u}{\sqrt{z}} \tag{4.14}$$

and the q_1q_2 rapidity with respect to the pp c.m.s. is

$$y_P = \ln \frac{x}{\sqrt{\tau}} \tag{4.15}$$

The rapidity cut that we adopt for the result presented below is

$$y_{MAX} = 1.5, \tag{4.16}$$

tighter than that used in some of the literature. Since the W and Z decay products may "migrate" as much as one rapidity unit, our cut means that they will fall within the observable range of ± 2.5.

4.3 Strong VV Amplitudes.

The object of interest in Eq. (4.11) is the VV scattering cross section, $\sigma(V_1V_2 \to V_1'V_2')$. Lacking both a good candidate for the relevant strong interaction theory and the techniques to compute the strong scattering amplitudes even if we did know the theory, we cannot make precise quantitative predictions. Our goal is more modest: to establish the order of magnitude of the signals to be expected if the VV scattering occurs by strong interactions.

To this end we have concentrated on two simple models of the strong VV amplitudes. One is motivated by the low energy theorems, discussed in Section 3,

which follow rigorously from global chiral $SU(2)$ symmetry. The other is the standard model taken in tree approximation, with the Higgs boson mass set to the value, $m_H = 1\ TeV$, at which partial wave unitarily implies the onset of strong interactions.[2] With these models we have computed the cross sections to produce the six diboson channels – $ZZ, W^+Z, W^-Z, W^+W^-, W^+W^+, W^-W^-$ – at four pp center of mass energies, $\sqrt{s} = 10, 20, 30, 40\ TeV$. For comparison we have also considered some dynamical models in particular cases: (1) scaling the measured $\pi\pi$ s–wave amplitudes by v/F_π,[13] (2) an $O(N)$ model of the Higgs sector solved to leading order in $1/N$,[21] and (3) pair production mediated by techni-rho production[24] in $SU(N)_{TC}$ technicolor models.

We begin by considering the scattering amplitudes for two longitudinally polarized gauge bosons in the standard model. As discussed in Section 2, up to corrections of order M_W^2/s which we neglect, these are equal to the scattering amplitudes for the corresponding unphysical Goldstone bosons w and z. The tree amplitude for $W_L^+W_L^- \to Z_LZ_L$ is then well approximated at high enough energy by the corresponding tree amplitude for $w^+w^- \to zz$. The latter is given by the sum of the two Feynman diagrams shown in Figure (5),

$$\begin{aligned} \mathcal{M}(w^+w^- \to zz) &= -2i\lambda - 4i\lambda^2 v^2 \frac{1}{s - m_H^2} \\ &= -2i\lambda \frac{s}{s - m_H^2} \end{aligned} \tag{4.17}$$

using the relationship between the quartic coupling constant λ and the vev v

$$\lambda = \frac{m_H^2}{2v^2} = \frac{G_F m_H^2}{\sqrt{2}} \tag{4.18}$$

In the limit $s \ll m_H^2$ the amplitude (4.17) approaches the value

$$\mathcal{M}(w^+w^- \to zz) \cong 2i\lambda \frac{s}{m_H^2} = i\frac{s}{v^2} \tag{4.19}$$

as required by the low energy theorems discussed in Section 3. While Eq. (4.17) is a perturbative result, Eq. (4.19) is valid to all orders in λ.

We have so far neglected Γ_H, the Higgs width. In the absence of a fourth generation of fermions, the dominant decays are to w^+w^- and zz, implying

$$\begin{aligned} \Gamma_H &\cong \frac{3\sqrt{2}}{32\pi} G_F m_H^3 \\ &\cong \frac{1}{2} \cdot \left(\frac{m_H}{1TeV}\right)^3 TeV \end{aligned} \tag{4.20}$$

For $m_H = 1\ TeV$, we have $\Gamma_H \cong \frac{1}{2}\ TeV$, a value so large that it calls into question the possibility of a simple particle interpretation. For such large values m_H must be regarded as a parameter of the Lagrangian rather than the mass of a well defined particle. If the theory exists for such large m_H, we have yet to determine the nature of its particle spectrum.

For our phenomenological estimates we wish to include the effect of Γ_H. If we simply modified the propagator in Figure (4b) with the replacement

$$\frac{1}{s - m_H^2} \to \frac{1}{s - m_H^2 + im_H\Gamma_H}$$

then the resulting amplitude

$$-2i\lambda \cdot \frac{s + im_H\Gamma_H}{s - m_H^2 + im_H\Gamma_H}$$

would not have the correct low energy limit, Eq. (4.19). We therefore adopt the following minimal prescription, which preserves analyticity and the constraints of the chiral $SU(2)$ symmetry: in Eq. (4.17) we give the pole its proper complex value and we rescale the amplitude by a complex constant to ensure the correct threshold behavior. The result of this prescription is the following list of amplitudes:

$$\mathcal{M}(w^+w^- \to zz) = -2i\lambda\left(1 - i\frac{\Gamma_H}{m_H}\right)\frac{s}{s - m_H^2 + im_H\Gamma_H} \tag{4.21a}$$

$$\mathcal{M}(wz \to wz) = -2i\lambda\left(1 - i\frac{\Gamma_H}{m_H}\right)\frac{t}{t - m_H^2 + im_H\Gamma_H} \tag{4.21b}$$

$$\mathcal{M}(w^+w^- \to w^+w^-) = -2i\lambda\left(1 - i\frac{\Gamma_H}{m_H}\right)\left\{\frac{s}{s - m_H^2 + im_H\Gamma_H} + \frac{t}{t - m_H^2 + im_H\Gamma_H}\right\} \tag{4.21c}$$

$$\mathcal{M}(w^+w+ \to w^+w^+) = \mathcal{M}(w^-w^- \to w^-w^-)$$
$$= -2i\lambda(1 - i\frac{\Gamma}{m_H})\{\frac{u}{u - m_H^2 + im_H\Gamma_H} + \frac{t}{t - m_H^2 + im_H\Gamma_H}\} \tag{4.21d}$$

$$\mathcal{M}(zz \to zz) = -2i\lambda(1 - i\frac{\Gamma_H}{m_H})$$
$$\{\frac{s}{s - m_H^2 + im_H\Gamma_H} + \frac{t}{t - m_H^2 + im_H\Gamma_H} + \frac{u}{u - m_H^2 + im_H\Gamma_H}\} \tag{4.21e}$$

These amplitudes with $m_H = 1\ TeV$ and $\Gamma_H = 0.48\ TeV$ define our first model for estimating yields of strongly interacting VV pairs in pp collisions.

Since the tree amplitudes respect the global chiral symmetry of the model, their low energy limits are as given by the low energy theorems. The low energy limits of Eqs. (4.21) are therefore valid to all orders in the strong coupling λ. The low energy amplitudes are

$$\mathcal{M}_1 \equiv \mathcal{M}(w^+w^- \to zz) \cong i\frac{s}{v^2} \tag{4.22a}$$

$$\mathcal{M}_2 \equiv \mathcal{M}(w^\pm z \to w^\pm z) \cong i\frac{t}{v^2} \tag{4.22b}$$

$$\mathcal{M}_3 \equiv \mathcal{M}(w^+w^- \to w^+w^-) \cong -i\frac{u}{v^2} \tag{4.22c}$$

$$\mathcal{M}_4 \equiv \mathcal{M}(w^+w^+ \to w^+w^+) \cong \mathcal{M}(w^-w^- \to w^-w^-) \cong -i\frac{s}{v^2} \tag{4.22d}$$

$$\mathcal{M}_5 \equiv \mathcal{M}(zz \to zz) \cong 0 \tag{(4.22e)}$$

The amplitudes (4.22) will be a valid description of longitudinal gauge boson scattering if s is large enough that the theorem of Section 2 applies ($w \sim W_L$, $z \sim Z_L$) but small enough that the low energy theorems of Section 3 are valid. We sometimes refer to this as the region of the "Fermi limit" since it is like the low energy regime of growing amplitudes that occurs in weak interactions at energies below the

masses of the mediating particles – W and Z for the weak interactions or the new spectrum of strongly interacting particles for the case we consider here.

Smooth extrapolation of the amplitudes (4.22) to larger s defines a minimal model, since the threshold behavior will continue smoothly until dynamical structures, such as resonances, are encountered. However we cannot extrapolate the amplitudes (4.22) indefinitely since they would eventually grow beyond the magnitude allowed by partial wave unitarily. We therefore adopt a simple prescription in the spirit of geometrical models of hadron scattering: we extrapolate the amplitudes (4.22) until the partial wave amplitudes saturate the unitarily bound while for higher energies we assume the partial wave amplitudes are at their maximally allowed values with the relative phases implied by (4.22). This is similar to geometrical models of strong interaction scattering, which assume that all classically allowed elastic partial waves contribute maximally. It yields a conservative estimate of the total cross section, in that we do not include contributions of higher partial waves beyond those s and p-wave amplitudes that contribute to (4.22) nor do we include the contributions of multibody final states.

The low energy amplitudes (4.22) are specified by three independent partial waves, $a_{JI}(s)$, constrained by unitarily to obey

$$| a_{JI}(s) | \leq 1. \tag{4.23}$$

Our model consists of taking the three indepent nonzero amplitudes to be

$$a_{00} = \frac{s}{16\pi v^2}\theta(16\pi v^2 - s) + \theta(s - 16\pi v^2) \tag{4.24a}$$

$$a_{02} = -\frac{s}{32\pi v^2}\theta(32\pi v^2 - s) - \theta(s - 32\pi v^2) \tag{4.24b}$$

$$a_{11} = \frac{s}{96\pi v^2}\theta(96\pi v^2 - s) + \theta(96\pi v^2 - s) \tag{4.24c}$$

The amplitudes (4.22) are then obtained from

$$\mathcal{M}_i = 16\pi i \sum_{J=0}^{1}(2J+1)(\cos\theta)^J A_J^i(s) \tag{4.25}$$

where the nonvanishing A^i_J are given by

$$A^1_0 = \frac{2}{3}(a_{00} - a_{02}) \tag{4.26a}$$

$$A^2_0 = \frac{1}{2}A^4_0 = a_{02} \tag{4.26b}$$

$$A^2_1 = A^3_1 = a_{11} \tag{4.26c}$$

$$A^3_0 = \frac{1}{3}(2a_{00} + a_{02}) \tag{4.26c}$$

It is easy to verify that for $s < 16\pi v^2$ Eqs. (4.24)-(4.26) are equivalent to the low energy amplitudes (4.22).

To judge the reliability of this approach we have considered two other unitary models for the $J = 0$ $w^+w^- \to zz$ amplitude. The first is based on a ϕ^4 field theory with a global, spontaneously broken $O(N)$ symmetry, which has been solved to leading order in $1/N$[21]. For $N = 4$ this model corresponds to the Higgs sector of the standard model, since $O(4)$ is homomorphic to $SU(2)$ x $SU(2)$. To leading order in $1/N$, $\mathcal{M}(w^+w^- \to zz)$ is, like the Born amplitude, pure s-wave, and is given by

$$\mathcal{M}(w^+w^- \to zz) = -2i\lambda\frac{s}{s(1+\Delta) - m_H^2} \tag{4.27}$$

where

$$\Delta(s) = \frac{N}{32\pi^2}\frac{m_H^2}{v^2}(1 - \ln\frac{-s}{M^2}) \tag{4.28}$$

and M is a renormalization scale which we will set to 1 TeV. Taking $m_H^2 \gg s$ and $N = 4$, we have

$$\mathcal{M}(w^+w^- \to zz) = i\frac{s}{v^2}[1 - \frac{s}{8\pi v^2}(1 + i\pi - \ln\frac{s}{M^2})]^{-1} \tag{4.29}$$

and

$$\sigma(w^+w^- \to zz) = \frac{s}{32\pi v^4}[(1 - \frac{s}{8\pi v^2}(1 - \ln\frac{-s}{M^2}))^2 + (\frac{s}{8\pi v^2})^2]^{-1} \tag{4.30}$$

Another alternative approach is based on rescaling measured pion scattering cross sections by

$$\sigma_{\pi^+\pi^-\to\pi^0\pi^0}(k) = \sigma_{w^+w^-\to zz}(\frac{v}{F_\pi}k) \tag{4.31}$$

where k is the pion center-of-mass momentum. Equation (4.31) is in fact a prediction of the $SU(3)_{TC}$ technicolor model. It was shown in Ref. 13 that the pion scattering cross section in Eq. (4.31) is reasonably well represented by the unitary parameterization

$$a_{JI} = \sin\delta_{JI}e^{i\delta_{JI}} \tag{4.33}$$

where

$$\delta_{00} = (a_{00})_{LET} \tag{4.33a}$$

$$e^{2i\delta_{02}} = \frac{1 + i(a_{02})_{LET}}{1 - i(a_{02})_{LET}}. \tag{4.33b}$$

Here $(a_{00})_{LET}$ and $(a_{02})_{LET}$ are the amplitudes predicted by the Low Energy Theorems, Eqs. (4.22),

$$(a_{00})_{LET} = \frac{s}{16\pi v^2} \tag{4.34a}$$

$$(a_{02})_{LET} = -\frac{s}{32\pi v^2} \tag{4.34b}$$

(compare Eqs. (4.24)). For the s-wave $w^+w^- \to zz$ cross section we have then

$$\sigma(w^+w^- \to zz)_{J=0} = \frac{32\pi}{9s} \mid a_{00} - a_{02} \mid^2 . \tag{4.35}$$

Finally, as an example of how resonances can contribute to the diboson yield, we consider techni-rho production by vector meson fusion with subsequent decay to a pair of longitudinally polarized vector bosons. For the $V_LV_L \to V_LV_L$ amplitudes we use an s-channel Breit-Wigner approximation, with techni-rho mass and width for an $SU(N)_{TC}$ technicolor theory given by[24]

$$m_{\rho_T} = \sqrt{\frac{3}{N}}\frac{v}{F_\pi} m_\rho \tag{4.36}$$

$$\Gamma(\rho_T \to V_LV_L) = (\frac{3}{N})^{3/2}\frac{v}{F_\pi}\frac{\Gamma(\rho \to \pi\pi)}{(1-4m_\pi^2/m_\rho^2)^{3/2}}. \tag{4.37}$$

Techni-rho production by vector meson fusion was previously computed in Ref. (13) but without including rapidity cuts on the final state bosons. Techni-rho production via $\bar{q}q$ annihilation was evaluated, with rapidity cuts, in Ref. (25).

4.4 Results and Discussion.

Our estimated yields of gauge boson pairs at pp colliders are obtained by substituting the strong VV amplitudes from the previous subsection into Eq. (4.11). We have used the quark distribution functions of Ref. (25) with $\Lambda = 200MeV$.[26] Yields are computed assuming an integreted luminosity of $10^{40}cm.^{-2}$, as would be achieved at a collider with a luminosity $\mathcal{L} = 10^{33}cm.^{-2}sec.^{-1}$ operating for $10^7sec. \cong \frac{1}{3}$ year. In all cases we impose a rapidity cut $\mid y_V \mid \leq 1.5$ on the produced gauge bosons. The rapidity cut helps to increase the ratio of VV pairs produced by new strong interactions relative to the $\bar{q}q \to VV$ "background" which has a large forward component, and it also ensures that the boson decay products are likely to fall within the experimentally observable solid angle. While we concentrate on the pp collider option, we have also considered $\bar{p}p$ collisions for a few cases; as discussed below, the differences in cross sections for pp and $\bar{p}p$ are not very great.

The level at which we can hope to detect new strong interactions by enhanced production of gauge boson pairs is determined by the size of the conventional pair production cross section via $\bar{q}q$ annihilation. The strong interaction mechanism produces only longitudinally polarized gauge bosons while those produced by $\bar{q}q$ annihilation are predominantly transverse. However since we have no efficient way

of measuring the boson polarizations we must consider the yield from $\bar{q}q \to VV$ for all polarizations. These yields are shown in Table 1, for four pp collider energies, $\sqrt{s} = 10, 20, 30, 40\ TeV$, and for diboson masses greater than 0.5, 1.0, and 2.0 TeV.[27] The yields fall very rapidly with increasing diboson mass.

Table 2 contains the yields obtained from the standard model amplitudes, Eq. (4.21), with $m_H = 1\ TeV$. Results are given for the six channels, ZZ, W^+Z, W^-Z, W^+W^-, W^+W^+, W^-W^-, with a diboson mass cut $m_{VV} > 1\ TeV$. Figures 6-11 show the corresponding mass distributions, dn/dm_{VV}, for m_{VV} from 0.5 to 2.0 TeV. The ZZ yield includes contributions from $zz \to zz$ and $w^+w^- \to zz$, while the W^+W^- yield includes contributions from $w^+w^- \to w^+w^-$ and $zz \to w^+w^-$. At the 40 TeV collider the ZZ and W^+W^- signals from Table 2 are both appreciably larger than the $\bar{q}q$ background yield from Table 1, for instance, 1100 ZZ pairs in the signal compared to 370 in the background. The ratios of yields, $W^+W^- : W^+Z + W^-Z : ZZ$, are also interesting since they are not sensitive to theoretical and experimental uncertainties in the absolute yields. For these ratios we find 4.3 : 1.8 : 1 for the $\bar{q}q$ background compared to 2 : 0.1 : 1 for the standard model signal. The smaller ratio for $W^+W^- : ZZ$ is characteristic of strong interaction models, while the WZ and like-sign WW ratios are more model dependent, as seen below. In our standard model example the W^+W^- and ZZ yields are much larger than those of the other four channels, because only they benefit from the $I = 0$ $s-$channel Higgs diagram. As is clear from Figs. 6-11, in this model the signal for $m_{VV} > 2\ TeV$ is negligible. However, in a more realistic model including a broad resonance at 1 TeV, we would not expect the total cross sections to be damped a la Breit-Wigner above resonance.

In Table 3 and Figs. 12-17 we exhibit the yields obtained from the model defined in eqs. (4.24)-(4.26), based on extrapolation of the amplitudes predicted by the low energy theorems.[28] In this case there are significant contributions for diboson masses above 2 TeV, and in Table 3 we present yields for both $m_{VV} > 1\ TeV$ and $m_{VV} > 2\ TeV$. For $\sqrt{s} = 40\ TeV$ and $m_{VV} > 1\ TeV$ the ratio $W^+W^- : W^+Z + W^-Z : ZZ$ is 1.3 : 1.4 : 1, compared to 4.3 : 1.8 : 1 for the $\bar{q}q$ background. In addition the model predicts large yields of like-sign dibosons, $W^+W^+ + W^-W^-$, a dramatic signature with no $\bar{q}q$ backgrounds. This model is intended to explore the possibility that the spectrum of new strongly interacting particles might lie well above 2 TeV, as may occur for example in ultracolor models.[5] The model treats the $I = 0, 1, 2$ channels "democratically" as prescribed by the low energy theorem, and therefore predicts large yields in the $W^\pm Z$ channels, with $I = 1, 2$, and in the pure $I = 2$ W^+W^+ and W^-W^- channels. As discussed in Section 4.3, we regard these yields as a lower limit

to the actual total yields, which would probably occur under such a hypothesis in additional partial waves and in higher multiplicity final states.

The bottom two rows of Table 3 show the yields for W^+W^+ and W^-W^- if the rapidity cut is relaxed from $\mid y_W \mid < 1.5$ to $\mid y_W \mid < 4$. The effect at $\sqrt{s} = 40\ TeV$ is to increase the yields by more than 50%. Since these charge $\pm$ 2 channels have no background from $\bar{q}q \to VV$, we can exploit the full solid angle coverage, which is likely to extend to $y = \pm 5$ for the decay products.[29]

In Table 4 and Figure 18 we compare the low energy theorem based model in the ZZ channel, Eqs. (4.24) -(4.26), with two unitary models which also satisfy the low energy theorems at threshold.* The first is the $O(N)$ φ^4 model solved to leading order in $1/N$ and then evaluated at $N = 4$,[21] Eq. (4.30), and the second is the scaled fit[13] to $\pi\pi$ scattering data, Eqs. (4.31)-(4.35). The models are in order of magnitude agreement for $m_{VV} < 2\ TeV$: they agree to 20% for $1/2 < m_{VV} < 2\ TeV$ and to 30 and 50% for $1 < m_{VV} < 1.8\ TeV$. However, they disagree in order of magnitude for $m_{ZZ} > 2\ TeV$. This is as we might expect since the models based on the pion data and the $1/N$ expansion each reflect only the two body, $J = 0$ channels. In a more complete description we would expect both higher partial waves and inelastic channels to set in at $m_{ZZ} \geq 2\ TeV$. We seek to model the effect of these additional contributions to the total cross section by the saturation prescription, Eq. (4.24), for the threshold amplitudes.

In Table 5 and Figs. 19-21 we show the results for techni-rho production by gauge boson fusion in $SU(N)_{TC}$ technicolor with $N = 2, 4, 6$. These results can be compared directly with the corresponding cross sections for techni-rho production by $\bar{q}q$ annihilation obtained in Ref. (25) for the case $N = 4$ and $\sqrt{s} = 40\ TeV$. From diboson fusion we find 380 ρ_T^0's and 690 $\rho_T^{\pm}$'s compared to 240 and 420 respectively from $\bar{q}q$ annihilation.

In Table 6 we compare pp and $\bar{p}p$ colliders at $\sqrt{s} = 10, 20, 30, 40\ TeV$. In particular we compute the ratios of pp to $\bar{p}p$ cross sections for production of ZZ pairs using the standard model with $m_H = 1\ TeV$, of Eq. (4.21), and the low energy amplitudes, Eq. (4.22). The difference is always less than 30%, and for 30 and 40 TeV it is less than 20%. Since pp colliders are likely to reach considerably greater luminosities than $\bar{p}p$ colliders, it is clear that the pp option is preferred.

We turn next to some estimates of what the total predicted yields may mean in

*In these models we have neglected the elastic ZZ contribution which vanishes in the low energy limit.

terms of observed events. We consider primarily leptonic decay channels, for which we expect detection efficiencies to be high and non-VV backgrounds to be very low. The results are summarized in Table 7. For instance, for the ZZ channel we consider the decay of one Z to $e^+e^-, \mu^+\mu^-$ while the other Z decays to $e^+e^-, \mu^+\mu^-$ or to $\bar{\nu}_e\nu_e, \bar{\nu}_\mu\nu_\mu, \bar{\nu}_\tau\nu_\tau$. We assume such decays could be reconstructed with efficiency ~ 1, so the "observability factor" in this case is just the net branching ratio, given by

$$B(Z \to \bar{e}e + \bar{\mu}\mu)(B(Z \to \bar{e}e + \bar{\mu}\mu) + 2B(Z \to \bar{\nu}\nu)) = .025.$$

The observability factor from WZ is computed similarly from the branching ratios for $Z \to \bar{e}e, \bar{\mu}\mu$ and $W \to e\bar{\nu}_e, \mu\bar{\nu}_\mu, \tau\bar{\nu}_\tau$. When no attempt is made to reconstruct the W charges, the WW channel is also reconstructed from the three leptonic modes $e\bar{\nu}_e, \mu\bar{\nu}_\mu, \tau\bar{\nu}_\tau$. Since the charge can probably be determined for muons as hard as 8 TeV but not for electrons without special effort,[29] the W^+W^+ / W^-W^- factor is just $(B(W \to \mu\bar{\nu}_\mu))^2$. A possible WZ channel which we have not included is $W \to \ell\nu + Z \to \bar{\nu}\nu$. If these decays could be reconstructed, the net observability factor for WZ in leptonic channels would increase significantly from the .015 shown in Table 7 to .06.

We have also included preliminary estimates for the channels VW and VZ, where V denotes either a W or Z decaying to $\bar{q}q$ jets. For these cases the observability factor is the product of branching ratios for the decays shown in the table multiplied by an "efficiency" factor or 0.2. The latter factor is based on an ISAJET study by E. Fernandez et al.,[30] which shows that hadronic decays can be distinguished from the QCD background of quark and gluon jets at a signal : noise level of 1 : 1 with efficiency 0.2.

These observability factors – and especially those involving hadronic decays – must be regarded at tentative estimates. The capability to detect W and Z's will benefit from the experience that will be acquired during the next ten years at CERN and FNAL. We anticipate that our estimates, based on the present, rather limited experience, will prove to be conservative.

In Tables 8 and 9 we exhibit the predicted yields of reconstructable events, based on the observability factors of Table 7. In Table 8 each pair of numbers represents the signal from the standard model (Table 2) compared to the $\bar{q}q$ annihilation background (Table 1), with $m_{VV} > 1\ TeV$ and $\mid y_V \mid < 1.5$. In Table 9 the signal

is taken from the extrapolated low energy theorem (Table 3); a second pair of numbers is given for $m_{VV} > 2\ TeV$, and the like-charge WW yields are shown both for $|\ y_W\ | < 1.5$ and $|\ y_W\ | < 4$.

Inspection of Tables 8 and 9 shows that it should be straightforward to detect the existence of strong interactions between W and Z bosons in a 40 TeV pp collider with luminosity approaching $10^{33} cm.^{-2} sec.^{-1}$. For instance, in both the models of Tables 8 and 9, the WW pairs detected in leptonic decays give a signal of order 100, representing a 10 σ enhancements above $\bar{q}q$ annihilation background. For the sum of ZZ and WZ detected leptonically,both tables 8 and 9 show $\sim 5\sigma$ enhancements over $\bar{q}q$ annihilation. Both tables also show large enhancements in the VW channels with V detected hadronically; for these cases a misidentification background equal to the signal must be added to the $\bar{q}q$ annihilation backgrounds shown in the table. For instance in Table 8 the VW signal of 180 is above a total estimated background of $180 + 140 = 320$, giving a 10σ enhancement. In addition the model of Table 9 contains some spectacular signals in the yields of dibosons with mass greater than 2 TeV and in the like-charge WW pairs.

From Tables 8 and 9 it is clear that neither the 10 nor 20 TeV collider would be sufficient to detect strong interactions among W's and Z's. Considering the uncertainties in the estimates of both signals and backgrounds, the expected yields and signal : noise ratios at 10 or 20 TeV do not allow unambiguous recognition of strong interaction enhancements. We show in Figs. 22-29 the total event yields expected for $\sqrt{s} = 30\ TeV$ and 40 TeV in our two strongly interacting models and with no strong interactions. The 30 TeV collider with $\mathcal{L} = 10^{33} cm.^{-2} sec.^{-1}$ is near the edge of what is required, and would also be inadequate if our estimates prove to be overly optimistic by as little as a factor 3.

It is also clear from these results that even for the 40 TeV collider it is important to approach as near as possible to the luminosity of $10^{33} cm.^{-2} sec.^{-1}$. Decreasing the assumed integrated luminosity by a factor 3, the $ZZ + WZ$ leptonic signals from Tables 8 and 9 go from $4.5 - 5.5\ \sigma$ down to $3.5 - 4.5\ \sigma$, the WW leptonic signal decreases from $8 - 14\ \sigma$ to $6 - 10\ \sigma$, and the VW hadronic signal goes from $8 - 10\ \sigma$ down to $4 - 6\ \sigma$. If the integrated luminosity is decreased by an order of magnitude, then the significance of the most prominent signals is diminished to the 2 or 3 σ level.

5. Multiple W and Z Production

In this section we shall briefly discuss mechanisms for multiple ($n > 2$) production of intermediate vector bosons. A high average multiplicity of W's and Z's in events with, say, a total transverse energy greater than $500\ GeV$ would be a clear signal for new strong interactions. Unfortunately, results based on the scaling properties of the effective chiral Lagrangian or on the resonance structure of technicolor models are not very encouraging. However, a rich resonance spectrum, somewhat different from that suggested by a technicolor rescaling of observed pion dynamics could modify the rather meager yields obtained below.

5.1 Vector meson fusion.

Multibody production rates via the fusion mechanism of Fig.1 are obtained by folding the effective vector boson luminosity, Eq. (4.6), into the cross section for $V_L V_L \to 2nV_L$. Since the equivalent strong scattering amplitude for $\varphi\varphi \to 2n\varphi$ conserves "parity" as defined in Section 3, only even numbers of longitudinally polarized vector bosons can be produced by this mechanism. The production of additional "soft" W_L's and Z_L's can be determined, using standard current algebra techniques, from the elastic and charge-exchange cross sections estimated in the previous section. The current algebra result can be estimated[6] by using massless $2n$-body phase space and a factor $\sqrt{\hat{s}}/v$ in amplitude for each additional W_L or Z_L, giving

$$\frac{\sigma(V_L V_L \to (2n+2)V_L)}{\sigma(V_L V_L \to 2nV_L)} \simeq \left(\frac{\hat{s}}{16\pi^2 v^2}\right)^2 \frac{1}{(2n)^2(2n+1)(2n-1)}. \qquad (5.1)$$

As a measure of the accuracy of the estimate (5.1), it can be compared with the exact current algebra calculation[31] in the "Fermi Limit" $m_H >> \sqrt{\hat{s}}$. In this case[13] the exact and approximate results for $W^+W^- \to 2$ or $4W$'s differ by no more than 30% over the range $1\ TeV \leq \sqrt{\hat{s}} \leq 2.5\ TeV$. We therefore adopt (5.1) as a reasonable approximation. Using the two-body cross section estimates of Sect. 4, we predict on this basis more than * 70 four-body events (90% of which have invariant mass above 2 TeV) for an integrated luminosity of $10^{40} cm^{-2}$ for pp interactions at $\sqrt{s} = 40\ TeV$. Ten percent of these events will contain two or more bosons decaying leptonically, a spectacular signature.

*This estimate is a lower bound in that we do not include a combinatorial factor for 4-body charge channels. This factor is partically compensated by the fact that we have not rigorously imposed y-cuts on all 4 W's, but have simply folded the factor (5.1) into the appropriately cut 2-body yields of Section 4.

A larger four-body yield could occur if there were a resonance in the TeV mass region with appreciable couplings to both the two-body and four-body channels. This possibility has been investigated[13] in the context of technicolor models, where resonance widths and masses are predicted from pion resonance parameters using formulae analogous to Eqs. (4.36-37). This prescription gives, for example, a four-body $W^{\pm}$ yield of at most 20 events in a year's running at the SSC. This is because the lightest pion resonance with significant decay branching ratios to both two- and four-body final states scales according to Eq. (4.36) to a $\varphi\varphi$ resonance mass of $3\,GeV$ or more for $N \leq 7$, so that the effective vector boson luminosity is appreciable only over the lower mass tail of the resonance. For large N the resonance mass decreases, but its width decreases more rapidly, significantly damping the production cross section.

5.2 $q\bar{q}$ annihilation.

Light quark-antiquark annihilation into the eaten scalar equivalents of longitudinally polarized W's and Z's is mediated by the $s-$ channel exchange of transversely polarized gauge bosons (W_T, Z_T, γ) that couple weakly to the strongly interaction w, z system through the axial and vector currents, Eqs. (3.19) and (3.11). Since these weak couplings do not conserve "parity", an odd number of W_L's and Z_L's can be produced through couplings to the axial current. In the tree approximation to the standard model, the production of three longitudinally polarized vector bosons is governed by the physical Higgs exchange diagram of Fig. 30. For $m_H \simeq 1\ TeV$, this process is dominated by the production and decay of a quasi-real Higgs particle. For $m_H >> \sqrt{\hat{s}}$, the Born approximation reduces to an effective four-point coupling as determined by current algebra. The corresponding rates were estimated in Ref. 6, where it was found that a year's running at the SSC would yield a total of about 150 three-body events in all charge channels for $m_H \simeq 1\ TeV$, and about 50 events for $m_H >> \sqrt{\hat{s}}$. While these numbers, at least for on-shell Higgs production, do not appear prohibitively small, a subsequent study[32] of the rates for $q\bar{q}$ annihilation into three transversely polarized W's and Z's via conventional gauge couplings indicates that the "strong coupling" contribution to three-body W_L and Z_L will be buried under a "weak" gauge coupling background. At first sight this result is somewhat surprising, as the diagram of Fig. 30 involves only two weak vertices and one strong vertex (HV_LV_L), while the background amplitude requires three weak vertices. However, there are a large number of diagrams[32] that can contribute to the background process, as well as a large number of possible spin configurations in the final state, and these combinatorial factors apparently overcome the weaker

coupling strength.

Nevertheless, an observable excess of three-body final states over "gauge theory" background might occur if there were a 1^+ resonance in the $1-2\ TeV$ mass region. For example, the results of Ref. 6 also show that the pair production process $q\bar{q} \to W_L^+W_L^-$ via (equivalent scalar) coupling to the vector current gives a two-body production rate of longitudinally polarized W's that is an order of magnitude lower than the rate for transverse W production. (In this case both amplitudes are second order in the weak gauge coupling.) Nevertheless, technirho production via $q\bar{q}$ annihilation, which has a rate comparable to the vector boson rate presented in Sect. 4, yields[25] over 200 W^+W^- and over 400 WZ events above "gauge theory" background. If there were, for example, an analogue of the axial vector A-meson with a mass below two TeV one might expect a similar excess above background of three-body events. Again, this would provide an important signal for new strong interactions in the electroweak sector.

6. Concluding remarks

We have studied the general signatures for a strongly interacting W, Z system and estimated detectable yields based on the properties of such systems that naturally assure the observed W/Z mass ratio. In this sense our estimates may be considered as minimal expectations. Specific models may entail additional production mechanisms, such as the gluon-fusion mechanism of extended technicolor models that could significantly enhance multi W, Z yields.[33] Signatures might also be enhanced by a sufficiently low mass spectrum of resonances. Various theoretical techniques have been applied to the analysis of the large m_H limit of the standard model[34,35] and of various composite models[36] in attempts to predict the expected spectrum. It has even been speculated [37] that strongly bound W, Z composite states could occur with masses as low as a hundred GeV. Possibly observable new phenomena may also arise from quasi-stable non-trivial scalar field configurations.[38]

Clearly the physics of a strongly interacting vector boson system may be very rich. Our aim in this paper has been to establish the experimental conditions that will assure at the very least an answer to the question of whether electroweak symmetry breaking involves new strong interactions or whether it is implemented by a standard relatively light Higgs particle. We saw in Sect. 4 that this question can be answered by a hadron facility capable of detecting the excess of centrally produced high mass pairs of vector bosons that are predicted if these bosons have strong couplings. We found that the proposed SSC parameters, namely a center-of-mass energy of 40 TeV and a maximum luminosity of $10^{33}\,cm^{-2}\,sec^{-1}$, meet the requirements for detectablity. While the yields of higher multiplicity events obtained in Sect. 5 are rather meager, they should contribute a few spectacularly signed events at a facility with these parameters. We found that a center of mass energy of 20 TeV or less is inadequate for the purpose outlined above, while a 30 TeV facility with $\mathcal{L} = 10^{33}\,cm^{-2}\,sec^{-1}$ or a 40 TeV one with reduced luminosity would be marginal. It goes without saying that that highest achievable energy would provide the best chance for studying the dynamics of a strongly interacting W, Z system should this be the solution to the electroweak symmetry breaking puzzle chosen by nature.

Acknowledgments

We wish to thank S. Dawson and I. Hinchliffe for much advice and assistance. We are also grateful for helpful discussions with G. Chew , H. Harari, S. Loken, and B. Zumino. M.K.G. acknowledges the hospitality and support of the Institute for Theoretical Physics, Santa Barbara, CA, and of the Aspen Summer Institute.

References

1. M. Veltman, Acta Physica Polonica B8, 475 (1977).

2. B. W. Lee, C. Quigg and H. Thacker, Phys. Rev. D16, 1519 (1977).

3. B. Cox and F. Gilman, Proc. DPF Summer Study on the Design and Utilization of the SSC, Eds. R. Donaldson and J. Morfin (Fermilab 1985).

4. S. Weinberg, Phys. Rev. D13, 974 (1976) and Phys. Rev. D19, 1277 (1977); L. Susskind Phys. Rev. D20, 2619 (1979).

5. D. B. Kaplan and H. Georgi, Phys. Lett. 136B, 183 (1984). D. B. Kaplan, H. Georgi and S. Dimopolous, Phys. Lett. 136B, 187 (1984).

6. M. S. Chanowitz and M. K. Gaillard, Phys. Lett. 142B, 85 (1984).

7. D. Jones and S. Petcov, Phys. Lett. 84B, 440 (1979); R. N. Cahn and S. Dawson, Phys. Lett. 136B, 196 (1984). See also S. Dawson , Nucl. Phys. B29, 42 (1985), G. L. Kane, W. W. Repko and W. B. Rolnick, Phys. Lett. 148B , 367 (1984).

8. J. M. Cornwall, D. N. Levin and G. Tiktopoulos, Phys. Rev. D10, 1145 (1974).

9. C. E. Vayonakis, Lett. Nuovo Cimento, 17, 383 (1976).

10. T. Appelquist and C. Bernard, Phys. Rev. D22, 200 (1980); T. Applequist, in Gauge Theories and Experiments at High Energies. Eds. K. C. Bowler and D. G. Sutherland, (Scottish Universities Summer School in Physics, 1981) p. 385, and references therein.

11. P. Sikivie et al., Nucl. Phys. B173, 189 (1980).

12. M. K. Gaillard, in $p\bar{p}$ Options for the supercollider, p. 192 (1984); M. J. Schochet, ibid, p. 222 (1984).

13. M. K. Gaillard, in Proc. DPF Summer Study on the Design and Utilization of the SSC, Eds. R. Donaldson and J. Morfin (Fermilab, 1985).

14. K. Fujikawa, B. W. Lee and A. I. Sanda, Phys. Rev. D6, 2923 (1972).

15. B. Zumino, private communication and references therein.

16. C. Becchi, A. Rouet and R. Stora, Comm. Math. Phys. 42, 127 (1975). BRS invariance has been used previously to derive Ward identities for two-point functions: L. Baulieu and R. Coquereau, Annals of Phys. 140, 163 (1982).

17. See for example, J. Zinn-Justin in Trends in Elementary Particle Theory, Eds. J. Ehlers et al., Lecture Notes in Physics 37, Springer Verlag (Berlin, 1975).

18. M. Chanowitz, M. Furman and I. Hinchliffe, Nucl. Phys. B153, 402 (1979).

19. O. Alvarez, M. Claudson and R. Ingermanson; M. B. Gavela and J. Gunion, work in progress. See Ref. 13 for a discussion.

20. S. Weinberg, Phys. Lett. 17, 616 (1966).

21. M. Einhorn, Nucl. Phys. B246, 75 (1984); R. Casalbuoni, D. Dominici, and R. Gatto, Phys. Lett. 147B, 419 (1984).

22. S. Adler and R. Dashen, p. 220, Current Algabras (W. Benjamin, N. Y., 1968).

23. For an alternative and equivalent derivation see S. Dawson, op. cit.

24. S. Dimopolous, Nucl. Phys. 168, 69 (1968); S. Dimopolous, S. Raby, and G. Kane, Nucl. Phys. B182, 77 (1981).

25. E. Eichten, I. Hinchliffe, K. Lane, and C. Quigg, Rev. Mod. Phys. 56, 579 (1984).

26. In particular we used the QUARKDIST program written by I. Hinchliffe.

27. We thank Ian Hinchliffe for the results tabulated in Table 1, which were obtained from computations done for Ref. (25).

28. Figures 11-16 are actually based on the low energy theorem amplitudes, Eq. (4.22). Since the figures are for $m_{VV} < 2\ TeV$, they are essentailly indistinguishable from the saturated form of the model, Eqs. (4.25)-(4.27).

29. H. H. Williams, Report of the 4π Detector Group, Summary Report of the PSSC Discussion Groups (Eds. P. Hale and B. Winstein), June, 1984.

30. E. Fernandez et al, Proc. DPF Summer Study on the Design and Utilization of the SSC, Eds. R. Donaldson and J. Morfin (Fermilab 1985).

31. J. Ellis, contribution to Ref. 13.

32. M. Golden and S. Sharpe, HUTP-85/A018 and LBL-19431 (1985).

33. G. Segre, Phys. Lett. 150, 187 (1985).

34. R. N. Cahn and M. Suzuki, Phys. Lett. 134B, 115 (1984).

35. R. Casalbuoni, S. de Curtis, D. Dominici and R. Gatto, Universiyt of Geneva preprint UGVA- DPT 1985/02-456 (1985). P. Q. Hung and H. B. Thacker, FERMILAB-Pub-84/104-T (1984). I. Montvay, Phys. Lett. 150B, 441 (1985).

36. B. Schrempp and F. Schrempp, DESY preprint 84-117 (1984) and references therein.

37. M. Veltman, Phys. Letters 139B, 307 (1984); TASI Lectures in Elementary Particle Physics 1984, Ed. D. N. Williams (U. of Michigan 1985).

38. J. M. Gipson and H. C. Tze, Nucl. Phys. B183, 524 (1981); J. M. Gipson, Nucl. Phys. B183, 524 (1981); F. Klinkhamer and N. S. Manton, Phys. Rev. D30, 2212 (1984).

VV Yields: $\bar{q}q$ annihilation

$\sqrt{s}=$	10 TeV	20 Tev	30 TeV	40 TeV
ZZ	0.8, 40, 670	8, 150, 1800	18, 260, 2900	29, 370, 3600
W^+Z	1, 60, 940	10, 180, 2000	20, 290, 2700	30, 390, 3600
W^-Z	0.5, 30, 560	5, 110, 1400	10, 190, 2100	18, 280, 2800
W^+W^-	4, 190, 3300	30, 660, 7400	60, 1200, 11000	90, 1600, 14000

Table 1

Boson pair yield from $\bar{q}q$ annihilation for $10^{40} cm.^{-2}$ integrated luminosity and $|y_V| < 1.5$. The three values are for m_{VV} above 2.0, 1.0, and 0.5 TeV.

VV Yields: $m_H = 1\ TeV$

$\sqrt{s} =$	10 TeV	20 TeV	30 TeV	40 TeV
ZZ	30	250	610	1100
W^+Z	2	17	42	76
W^-Z	0.7	8	22	41
W^+W^-	61	500	1200	2200
W^+W^+	3	25	63	110
W^-W^-	0.5	5	17	33

Table 2

Yields of boson-boson pairs from boson-boson fusion computed in the standard model with $m_H = 1\ TeV$, for $10^{40} cm.^{-2}$ integrated luminosity and cuts of $m_{VV} \geq 1.0\ TeV$ and $\mid y_V \mid < 1.5$.

VV Yields: low energy theorem extrapolated

$\sqrt{s} =$	10 TeV	20 TeV	30 TeV	40 TeV
ZZ	0.4, 8	12, 88	50, 250	110, 470
W^+Z	1, 8	20, 80	80, 230	180, 440
W^-Z	0.3, 3	9, 36	36, 110	85, 230
W^+W^-	0.6, 12	16, 120	60, 330	140, 630
W^+W^+	1, 12	30, 110	110, 300	220, 560
W^-W^-	0.1, 2	5, 22	20, 74	50, 150
W^+W^+ $\mid y_W \mid < 4$	2, 15	40, 170	160, 490	340, 970
W^-W^- $\mid y_W \mid < 4$	0.1, 2	6, 33	30, 120	80, 260

Table 3

Boson-boson fusion yields from extrapolated (see text) low energy theorems, for $10^{40} cm.^{-2}$ integrated luminosity and, except for the last two rows, $\mid y_V \mid < 1.5$. The two entries are for m_{VV} above 2.0 and 1.0 TeV.

	Low Energy Thm.	$0(N)$ Model	Pion Data
$0.5 < m_{ZZ} < 2TeV$	690	560	560
$1.0 < m_{ZZ} < 1.8$	320	160	230
$m_{ZZ} > 2TeV$	110	13	14

Table 4

Yields of ZZ pairs for $\mid y_Z \mid < 1.5$ and $10^{40} cm.^{-2}$ integrated luminosity.

$N_{TC} =$	2	4	6
W^+Z	220	450	670
W^-Z	110	240	370
W^+W^-	180	380	570

Table 5

Boson pair yields from s-channel techni-rho formation in technicolor $SU(N)$ models with $N = 2,4,6$. Yields assume 10^{40} $cm.^{-2}$ integrated luminosity and cuts $\mid y_V \mid < 1.5$ and $m_{VV} > 1.0\ TeV$.

ZZ yields: pp versus $\bar{p}p$

$\sqrt{s} =$	$10\ TeV$	$20\ TeV$	$30\ TeV$	$40\ TeV$
$m_H = 1\ TeV$	0.8	0.9	0.9	1
Low Energy Thm.	0.7	0.7	0.8	0.8

Table 6

The ratio $\sigma(pp \to ZZ+\cdots)/\sigma(\bar{p}p \to ZZ+\cdots)$ computed from the double bremstrahlung mechanism using the standard model with $m_H = 1\ TeV$ and the low energy theorems to compute the gauge boson scattering amplitudes. We have imposed the cuts $\mid y_Z \mid < 1.5$ and $m_{ZZ} > 1.0 TeV$.

Net Observability Factors for Observable Modes

Boson Pair(s)	Decay Modes	Observability Factor
ZZ	$\bar{\ell}\ell + \bar{\ell}\ell/\nu\bar{\nu};\ \ell = e,\mu$	.025
WZ	$\ell' v + \bar{\ell}\ell;\ \ell' = e,\mu,\tau;\ \ell = e,\mu$	.015
$VZ:\ V = W + Z$	$\bar{q}q + \bar{\ell}\ell;\ \ell = e,\mu$	.009 $V = W$ .018 $V = Z$
$VW:\ V = W + Z$	$\bar{q}q + \ell\nu;\ \ell = e,\mu,\tau$	.075 $V = W$ .037 $V = Z$
WW	$\ell\nu + \ell\nu;\ \ell = e,\mu,\tau$	.063
W^+W^+/W^-W^-	$\mu^+\nu\mu^+\nu/\mu^-\nu\mu^-\nu$	.0069

Table 7

Net "observability factors" for some decays of two gauge bosons, as defined in the text.

Detectable VV yields: $m_H = 1\ TeV$

$\sqrt{s}=$ Boson Pair(s)	10 TeV	20 TeV	30 TeV	40 TeV
ZZ	0.8/1	6/4	15/6	28/9
WZ	.04/1	0.4/4	1/7	2/10
$VZ:\ V=W+Z$	0.6/2	5/5	12/9	21/13
$VW:\ V=W+Z$	5/18	41/60	100/110	180/140
WW	4/12	33/42	82/76	140/100
$W^+W^+ + W^-W^-$	.02	0.2	0.5	0.9

Table 8

Yields of VV pairs into reconstructable final states computed with "observability factors" from Table 7. The first entry is the signal from the standard model, $m_H = 1$, based on Table 2. The second entry is the background from $\bar{q}q$ annihilation, based on Table 1. Yields are for 10^{40} integrated luminosity, $\mid y_V \mid < 1.5$, and $m_{VV} > 1.0\ TeV$. The entries in rows three and four have additonal QCD backgrounds as discussed in the text.

Detectable VV yields: low energy theorem extrapolated

$\sqrt{s}=$	10 TeV	20 TeV	30 TeV	40 TeV
	.01/.02	0.3/0.2	1/0.5	3/0.7
ZZ	0.2/1	2/4	6/6	12/9
	.02/.02	0.4/0.2	2/0.5	4/0.7
WZ	0.2/1	2/4	5/7	10/10
	.02/.03	0.5/0.3	2/0.6	4/1
$VZ:\ V=W+Z$	0.2/2	3/5	8/9	14/13
	0.2/0.4	5/3	19/6	41/9
$VW:\ V=W+Z$	2/18	23/60	65/110	130/140
	0.1/0.3	3/2	12/4	26/6
WW	2/12	16/42	44/76	84/100
	.007	0.2	0.9	2
$W^+W^+ + W^-W^-$	0.1	0.9	2	5
$W^+W^+ + W^-W^-$	.01	0.3	1	3
$\mid y_W \mid < 4$	0.1	1	4	9

Table 9

VV yields to detectable final states, computed from "branching ratios times efficiencies" from Table 6. Top entries are signal/$\bar{q}q$ backgound for $m_{VV} > 2\ TeV$, bottom entries for $m_{VV} > 1\ TeV$. Yields assume $10^{40} cm.^{-2}$ integrated luminosity and $y_V < 1.5$. The entries in rows three and four have additional QCD backgrounds as discussed in the text.

Figure Captions

Figure 1 Two gauge boson production by boson–boson fusion.

Figure 2 Two gauge boson production by quark–antiquark annihilation.

Figure 3 Lowest order (a) and higher order corrections (b) to W self-energy.

Figure 4 Higgs production by diboson fusion.

Figure 5 Tree diagrams for $ww \to zz$.

Figure 6–11 Mass distribution of boson pairs computed from diboson fusion in the standard model with $m_H = 1\ TeV$. We impose a rapidity cut $| y_V | < 1.5$ and assume an integrated luminosity of $10^{40} cm.^{-2}$.

Figure 12–17 Mass distributions from diboson fusion assuming the model based on the low energy theorems. Rapidity cut and luminosity are as in fig. 6–11.

Figure 18 Comparison of the model based on the low energy theorem to the $O(N)$ model and the scaled pion–pion scattering data. Rapidity cut and luminosity are as in figs. 6–11.

Figure 19-21 Diboson fusion production of techni–rho which decays to gauge boson pairs, for $SU(N)_{TC}$, N = 2,4,6. Rapidity cut and luminosity are as in figs. 6–11.

Figure 22–20 Total boson pair yields as a function of invariant mass for $| y_V | < 1.5$ and an integrated luminosity of $10^{40}\ cm.^{-2}$. The distributions shown are for two strong interaction models and in the absence of strong interactions.

Figure 30 Tree amplitude for production of three longitudinally polarized gauge bosons by $\bar{q}q$ annihilation.

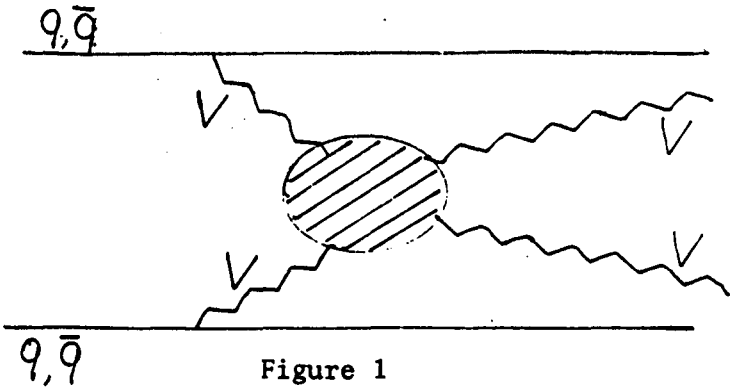

Figure 1

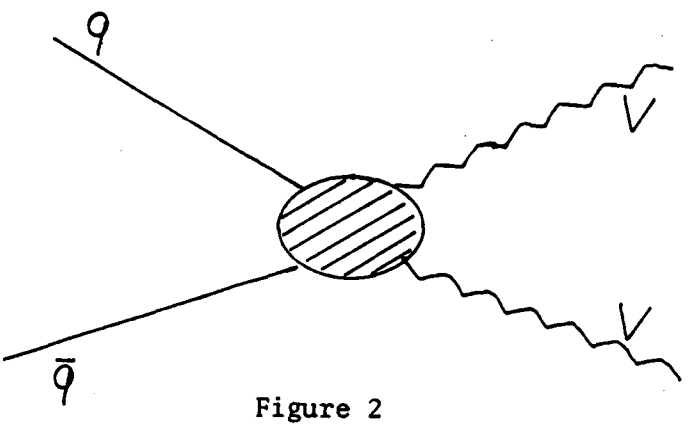

Figure 2

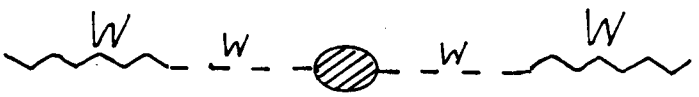

Figure 3a

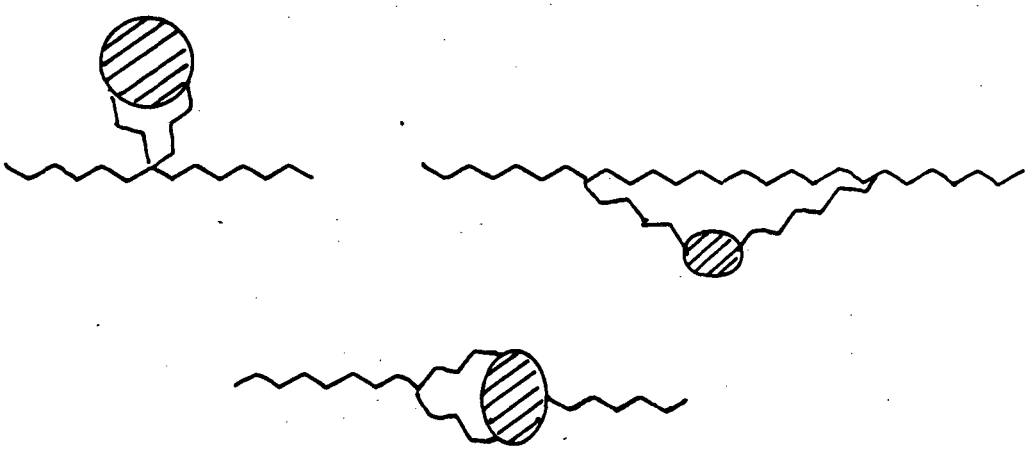

Figure 3b

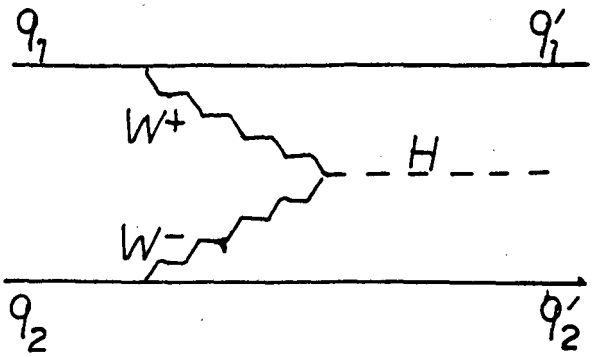

Figure 4

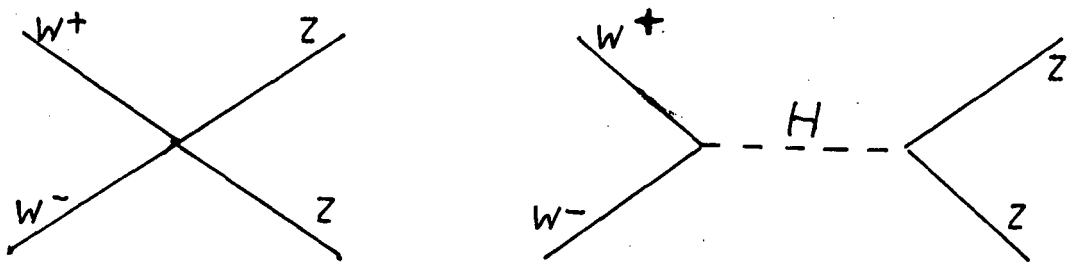

Figure 5

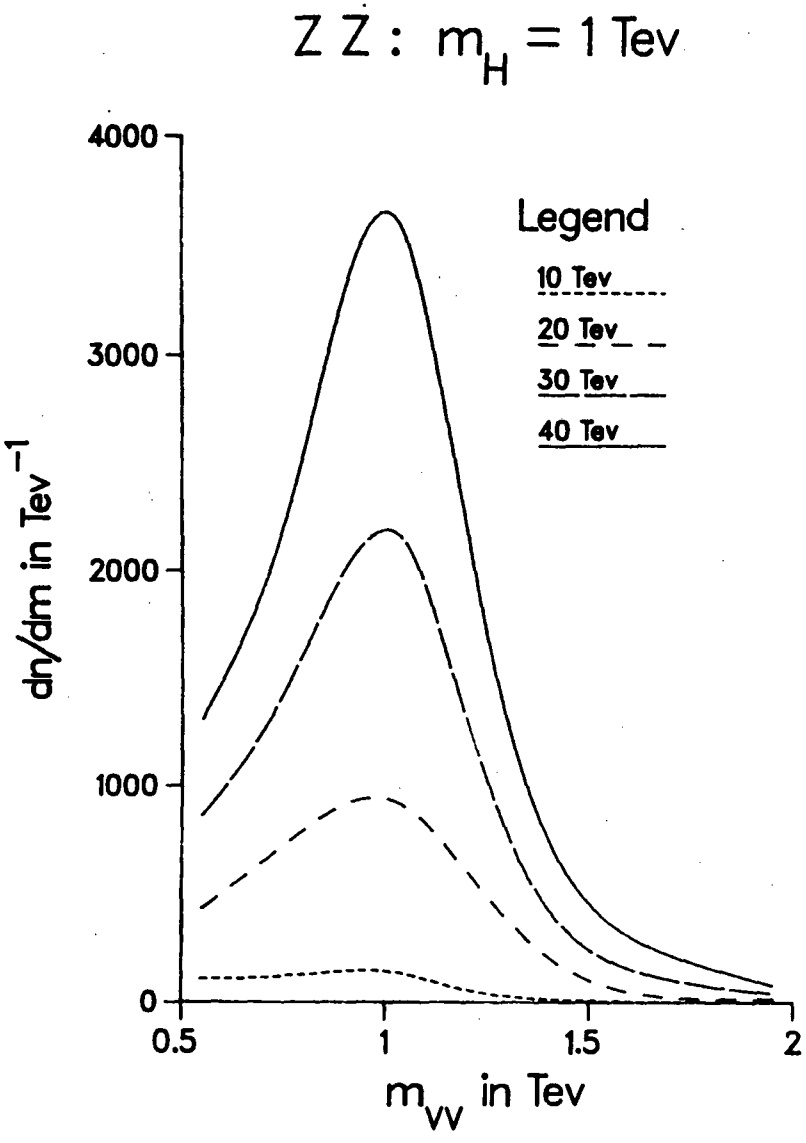

Figure 6

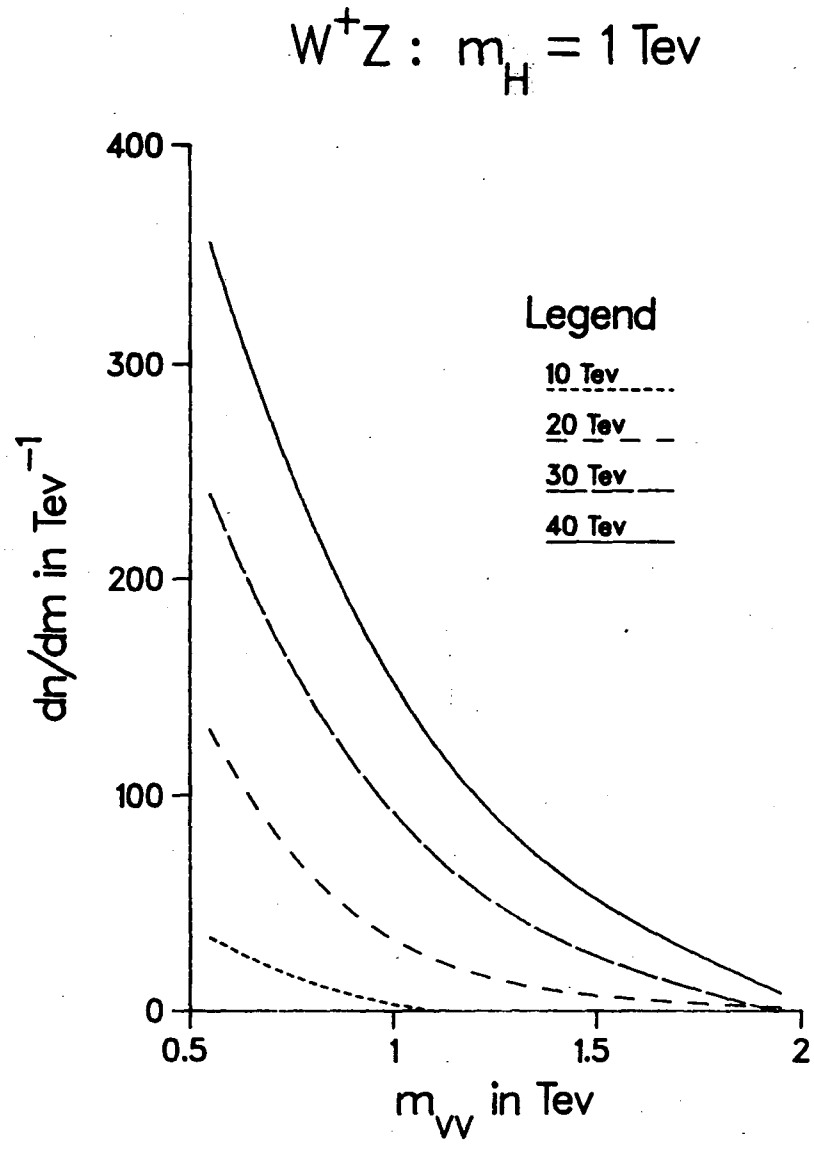

Figure 7

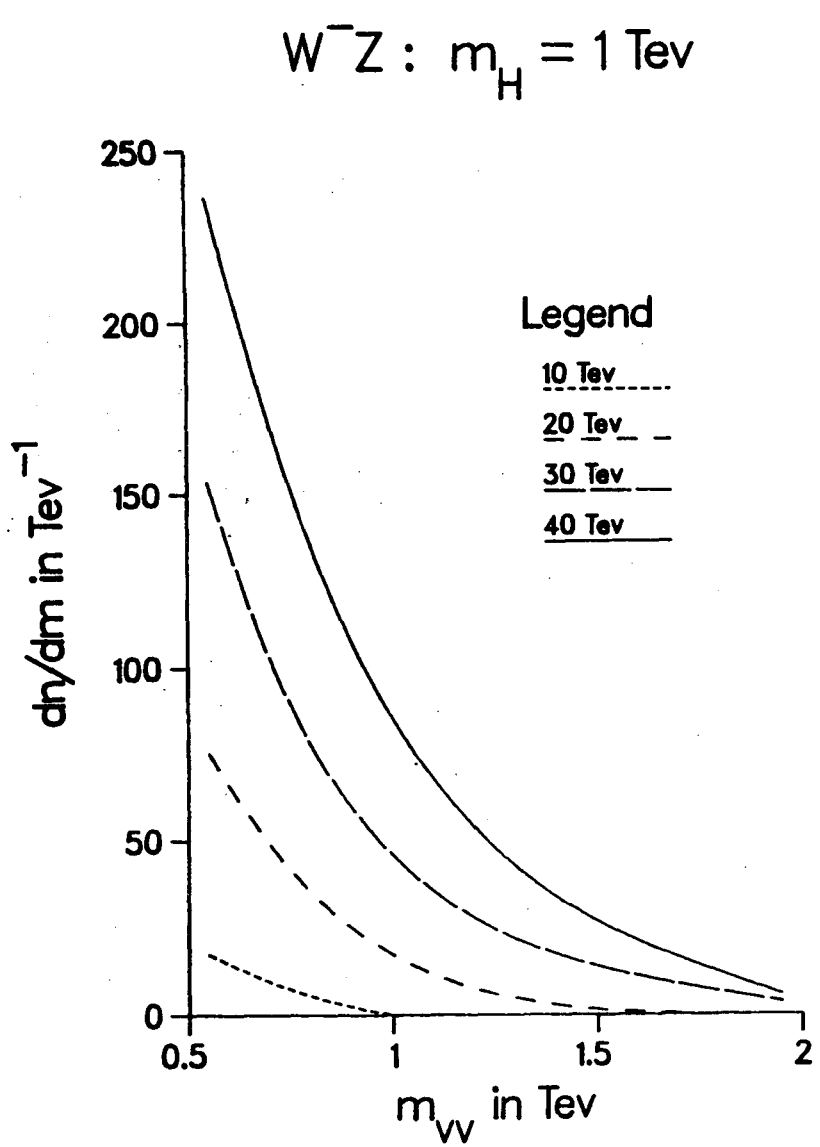

Figure 8

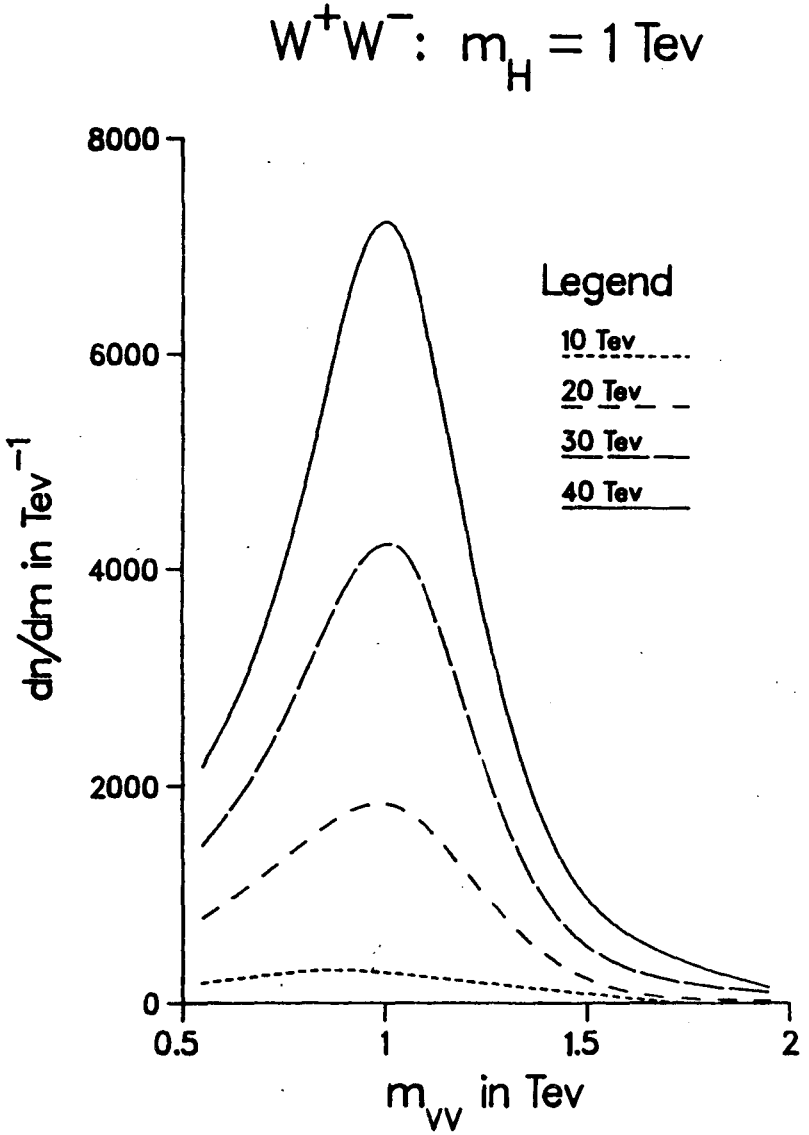

Figure 9

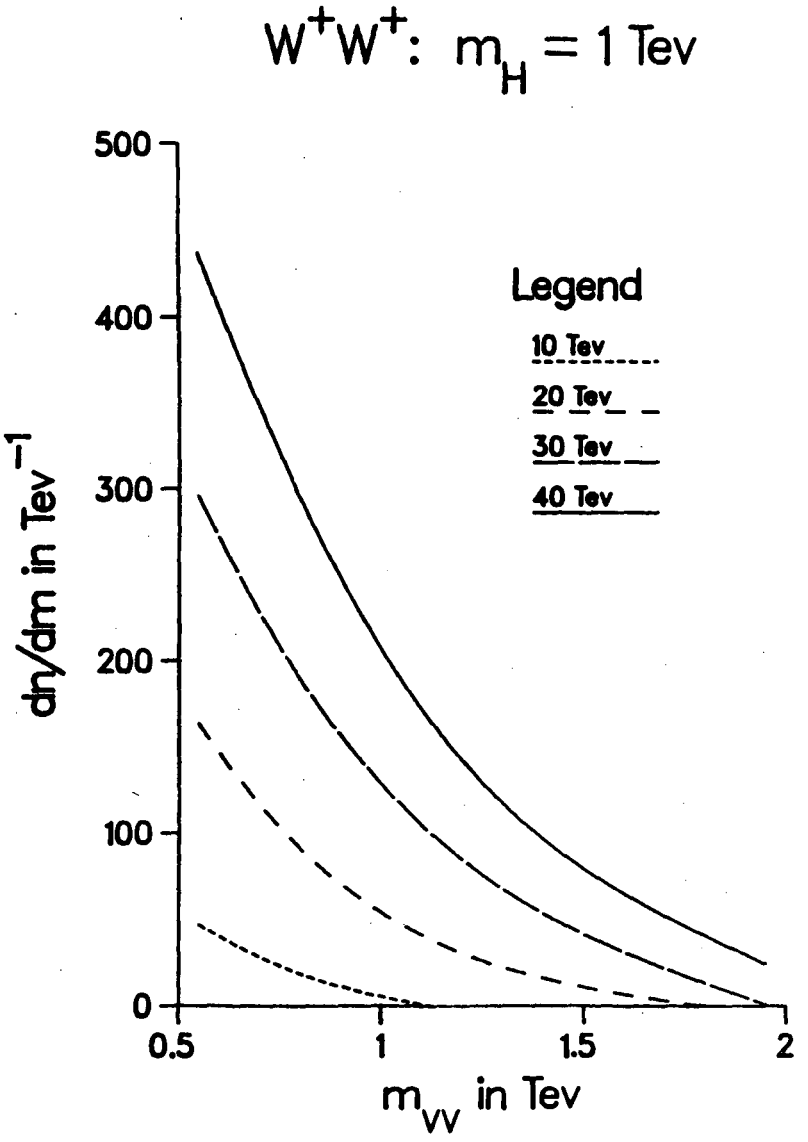

Figure 10

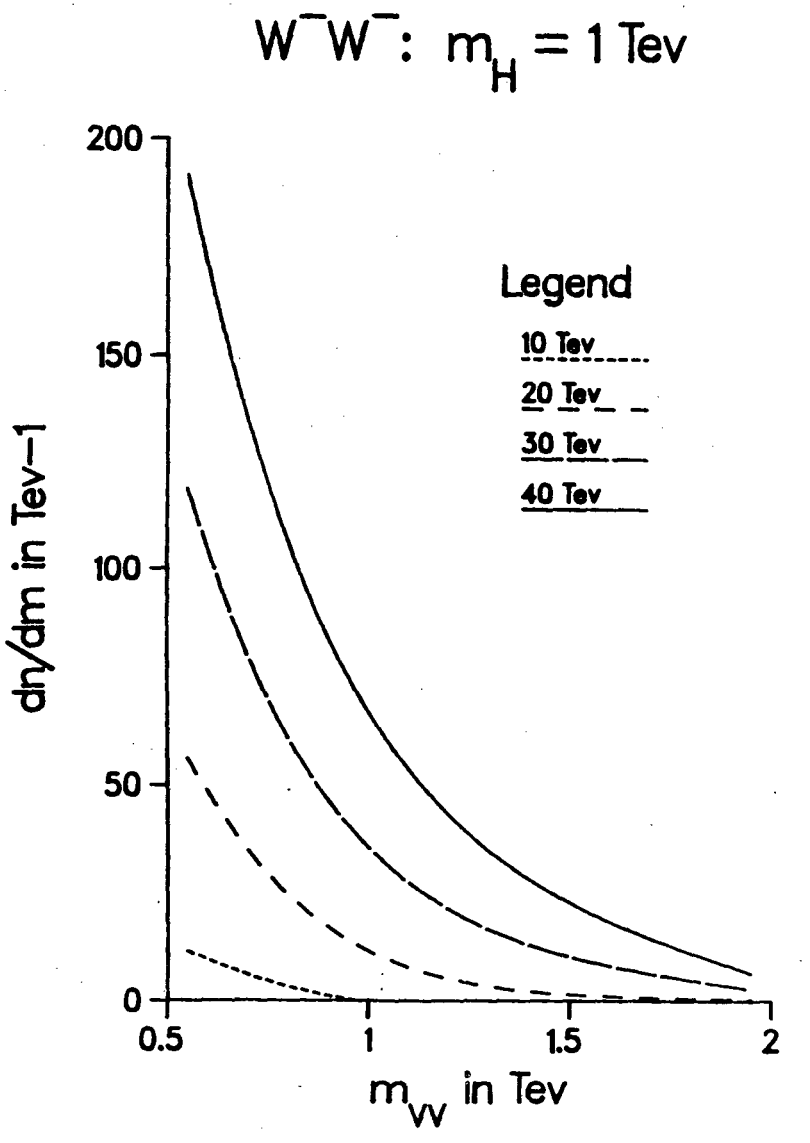

Figure 11

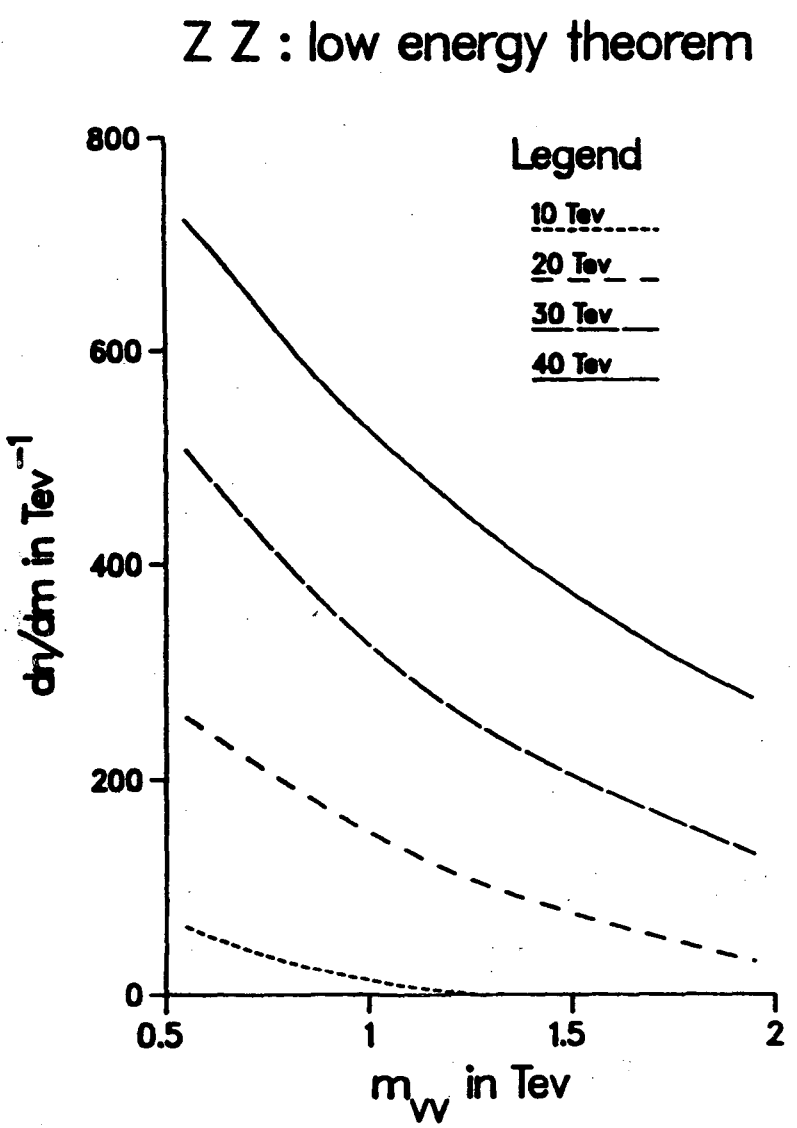

Figure 12

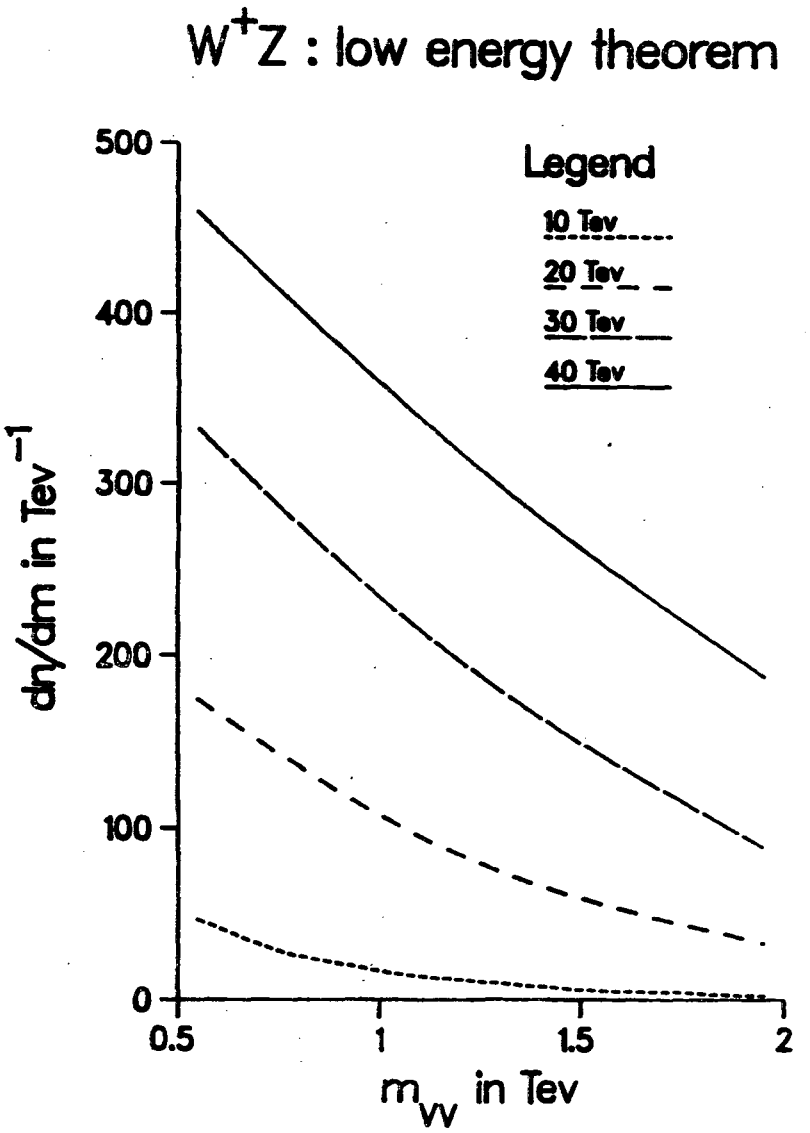

Figure 13

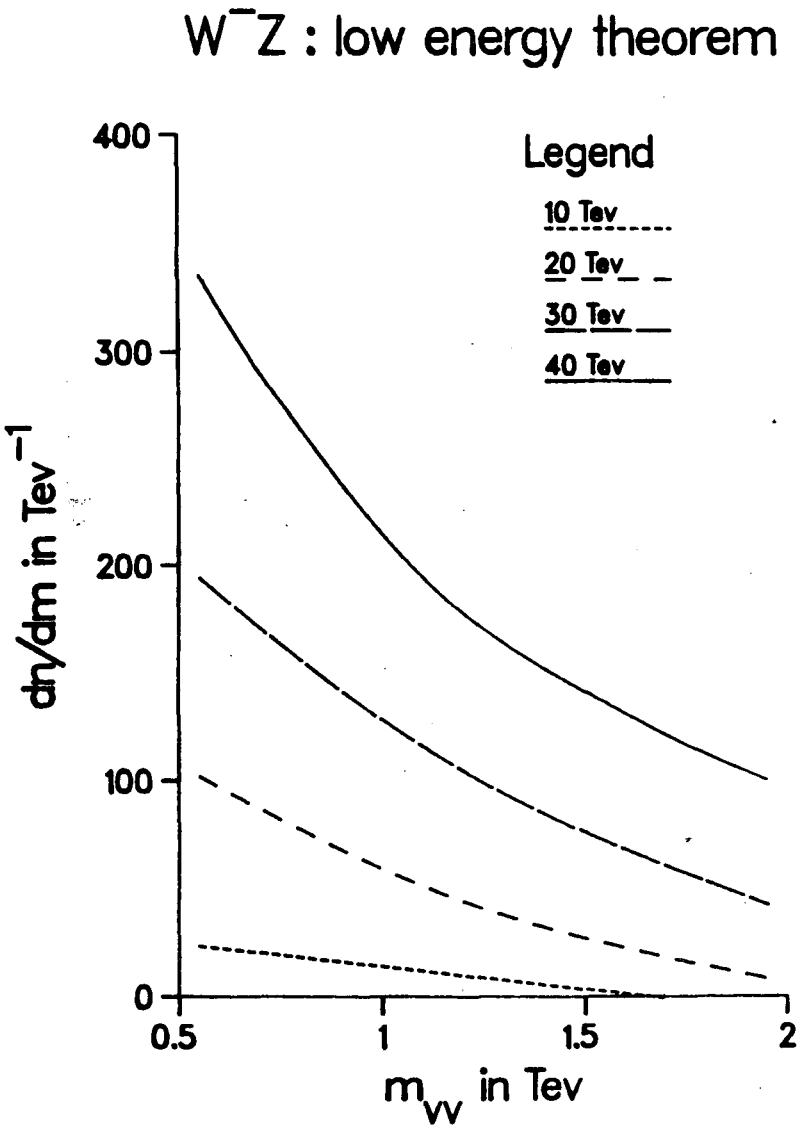

Figure 14

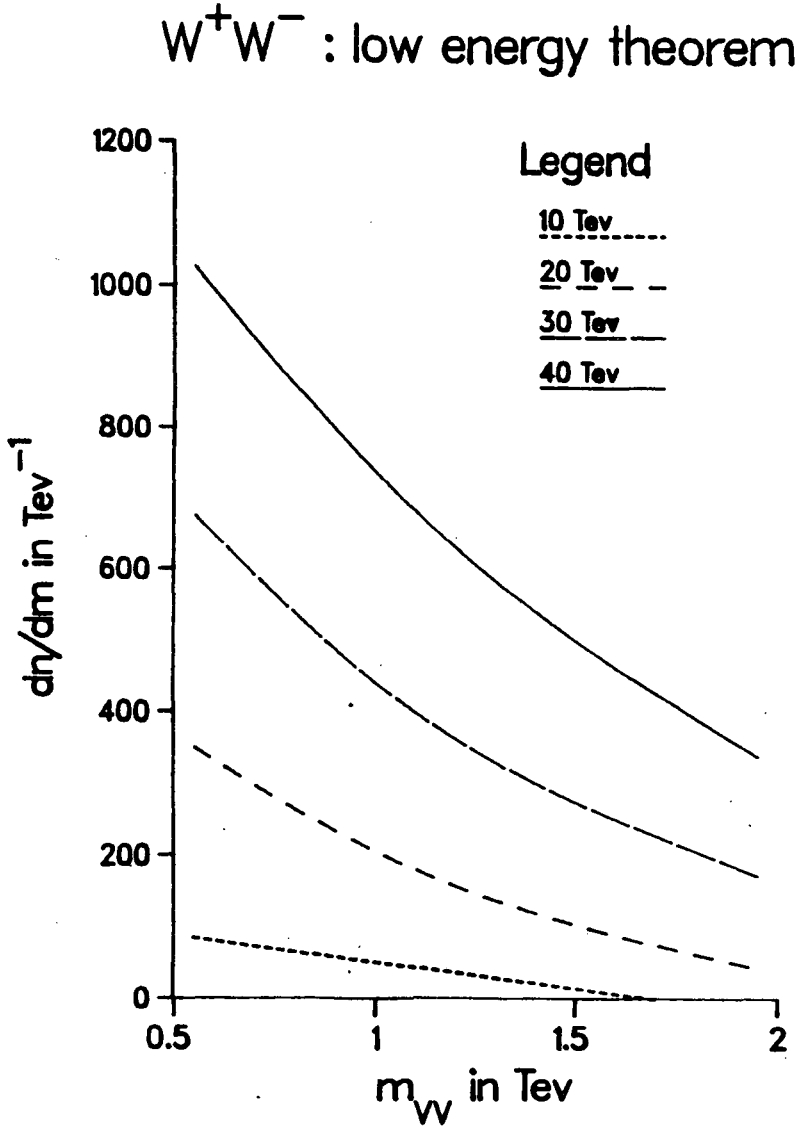

Figure 15

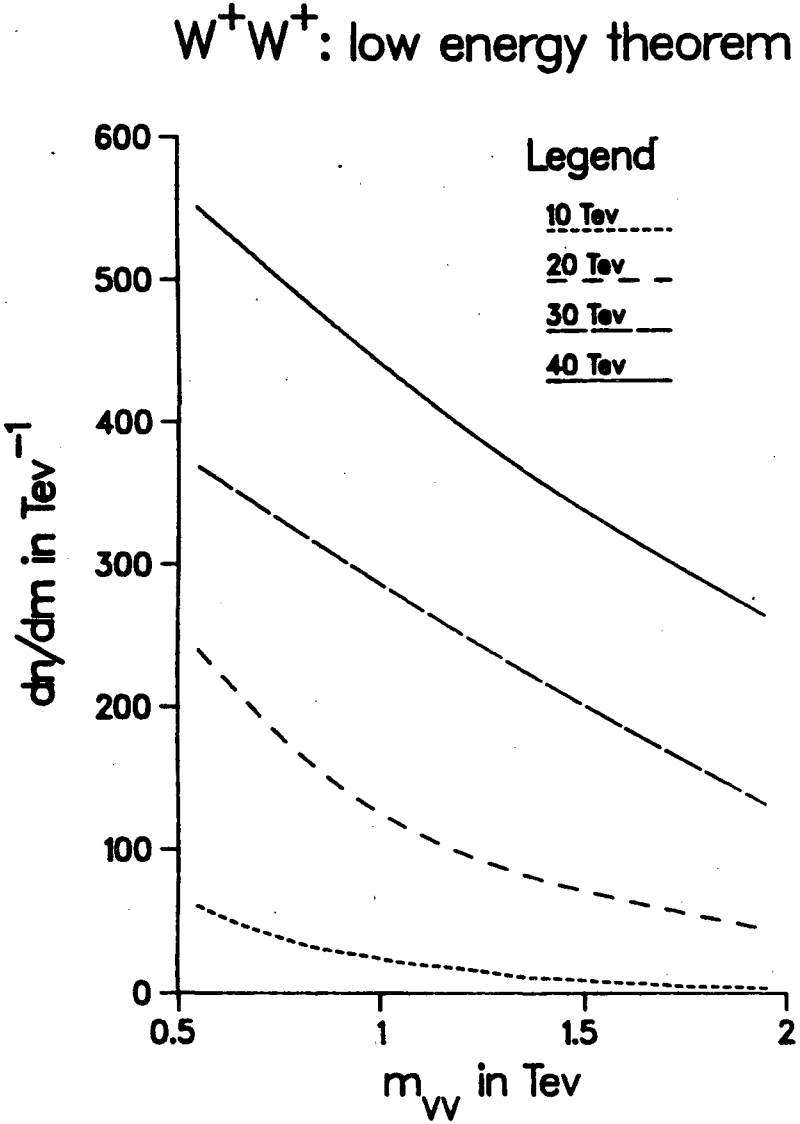

Figure 16

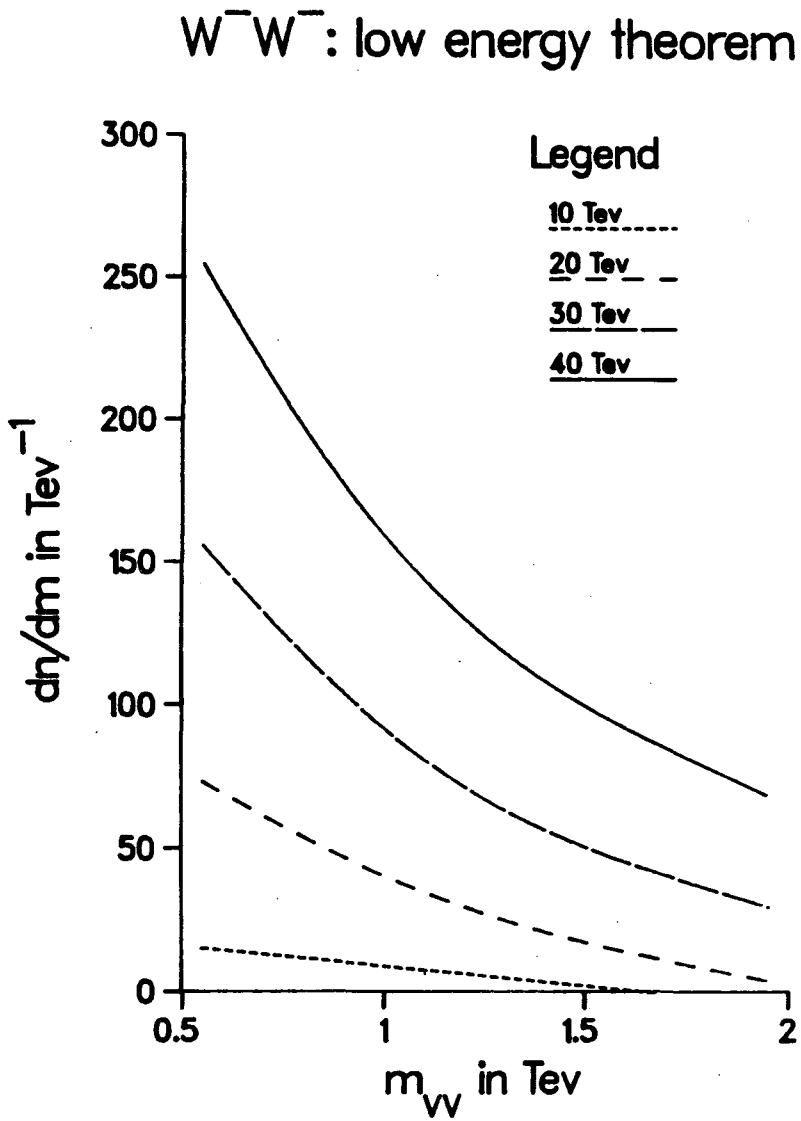

Figure 17

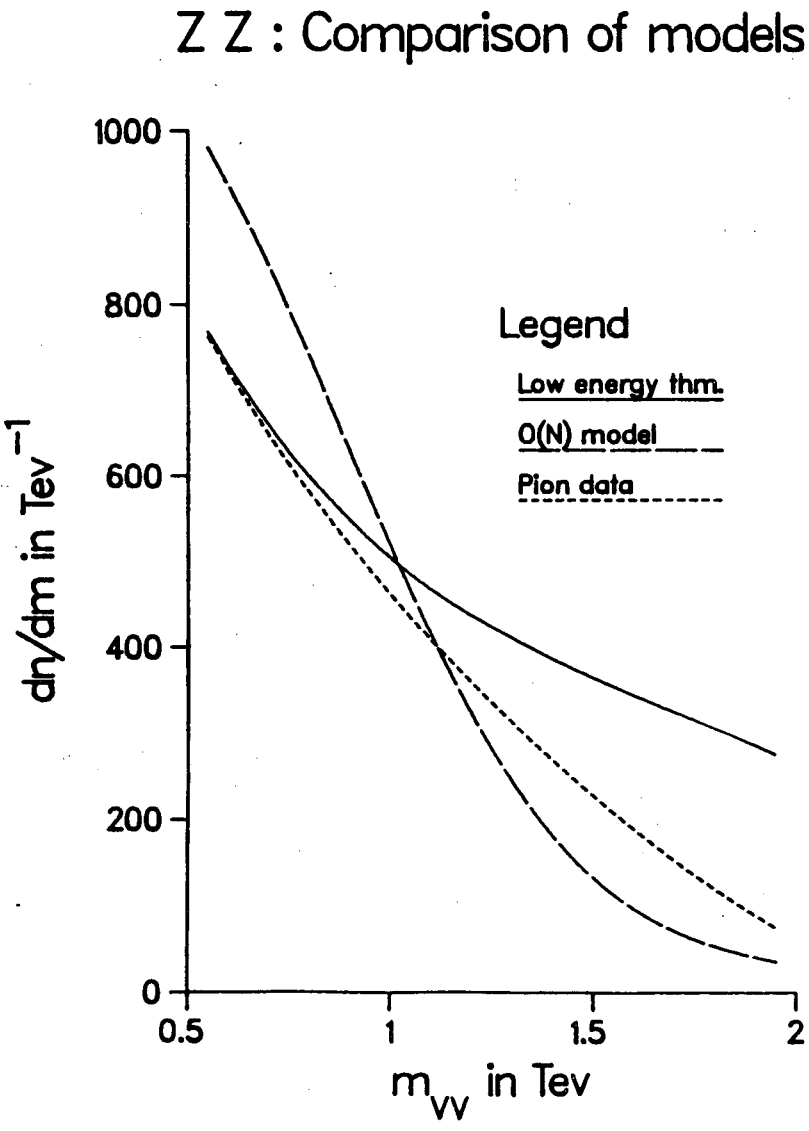

Figure 18

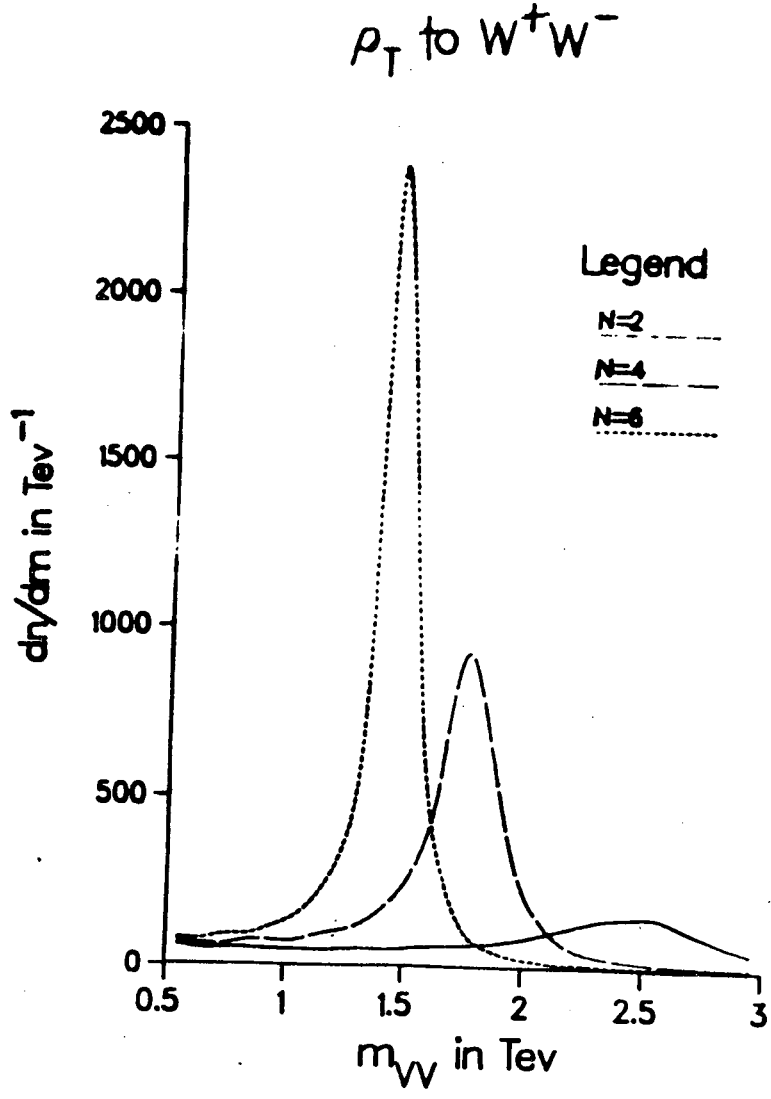

Figure 19

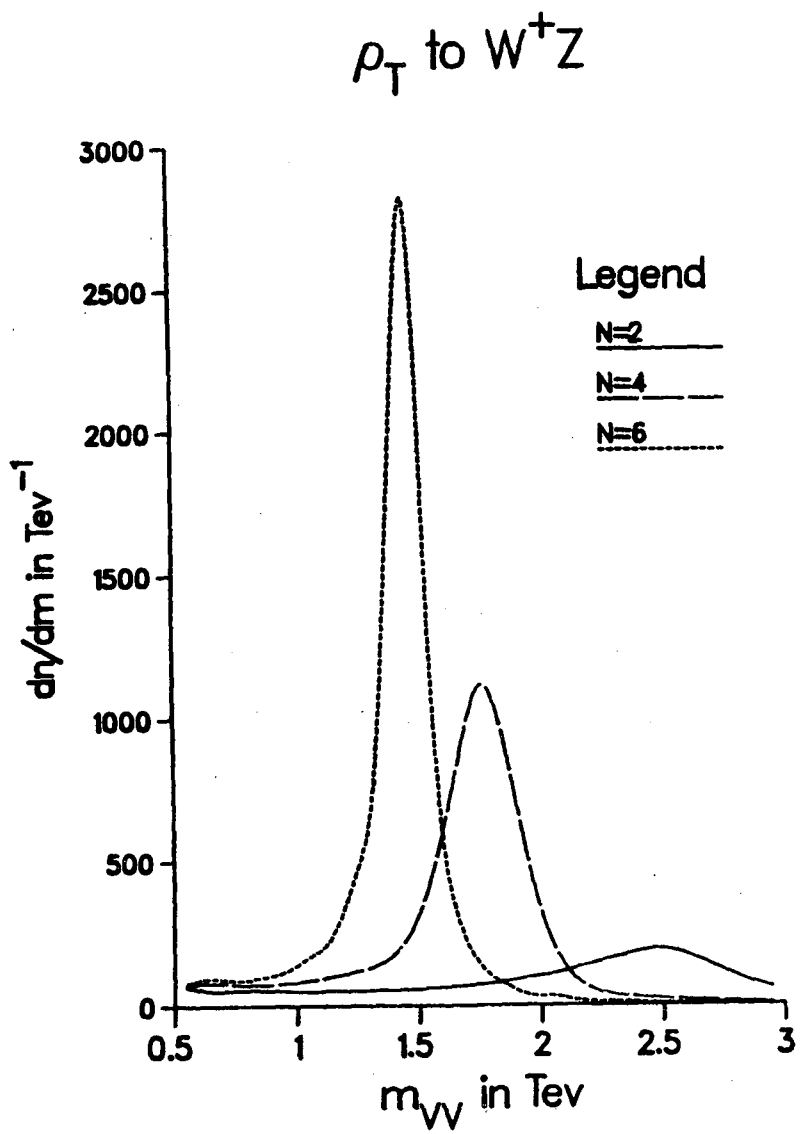

Figure 20

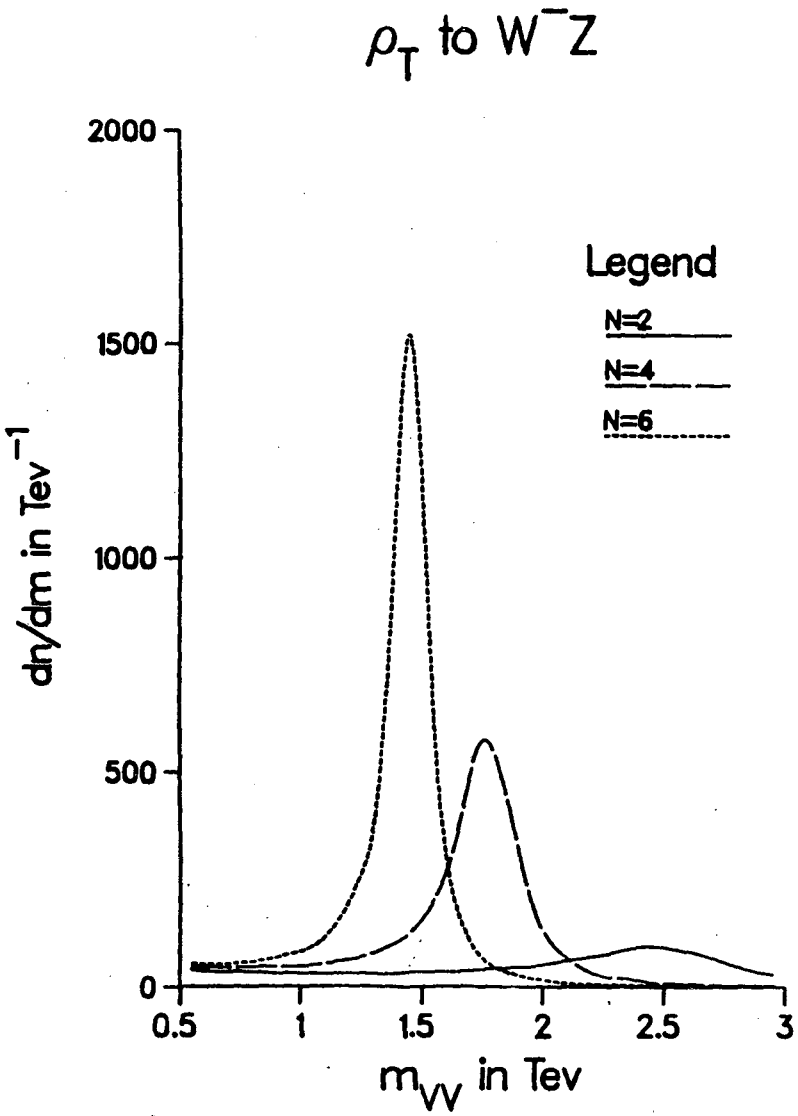

Figure 21

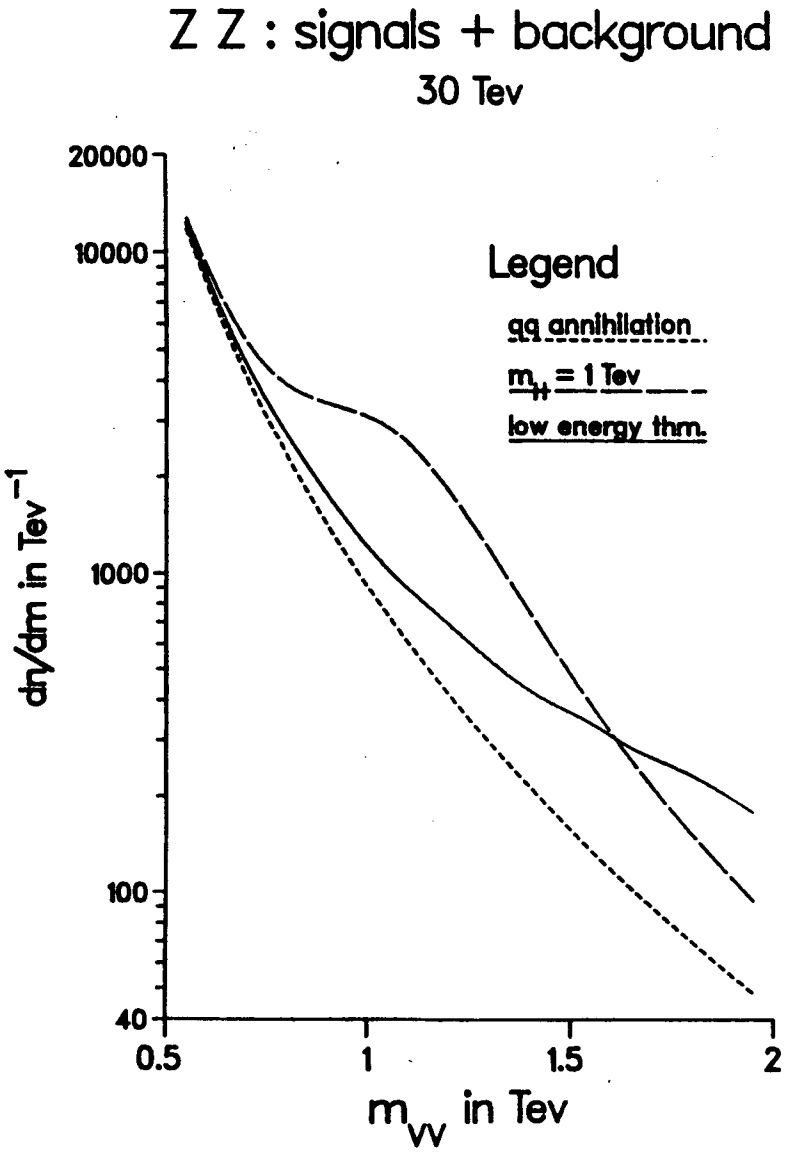

Figure 22

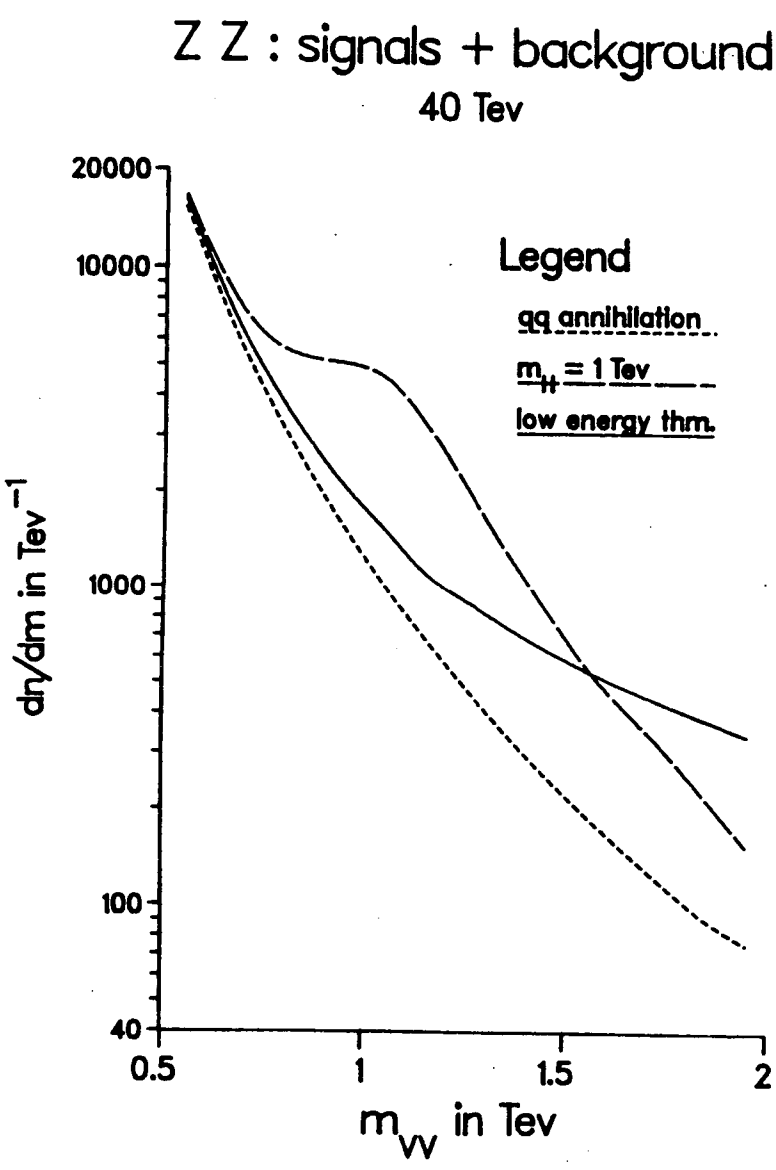

Figure 23

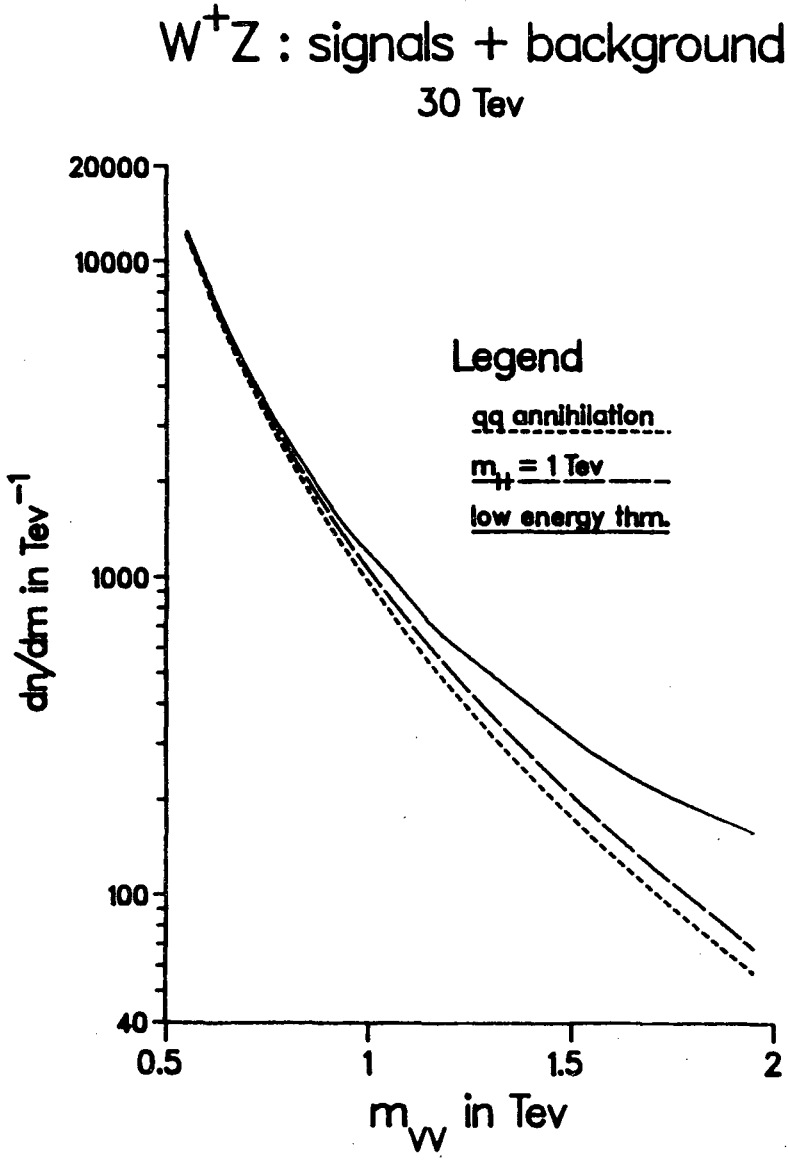

Figure 24

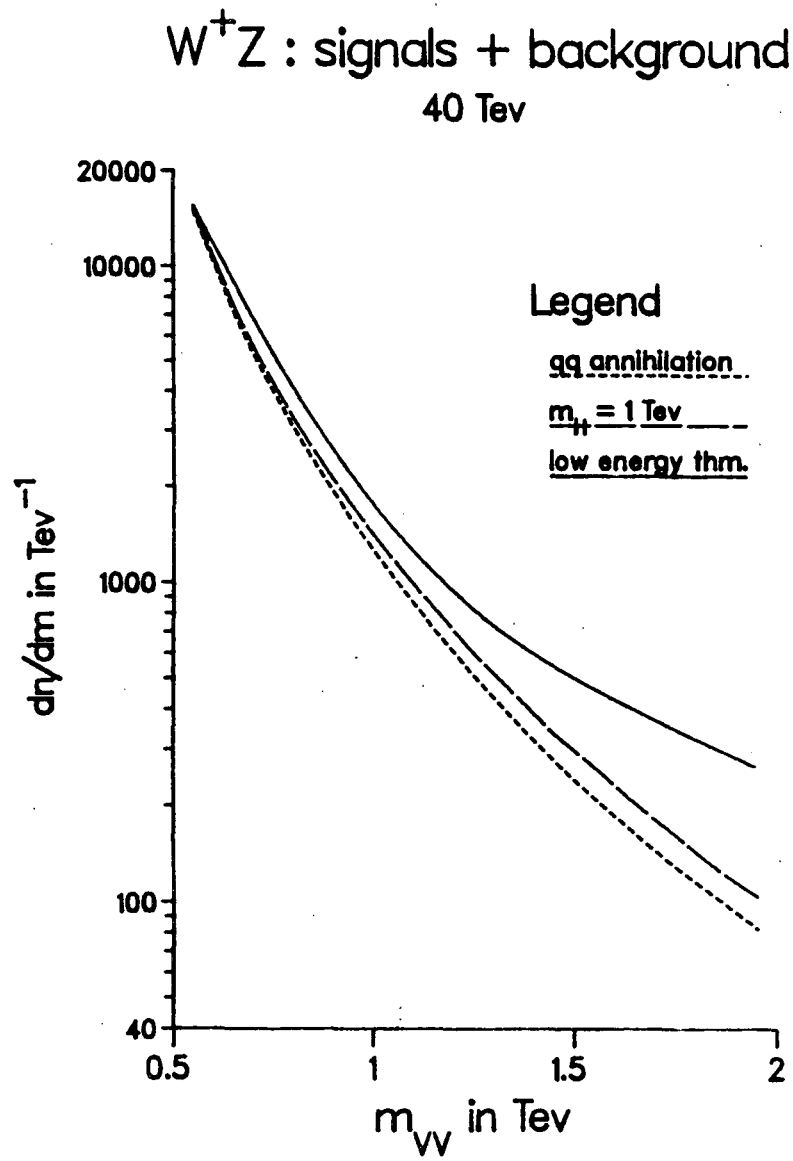

Figure 25

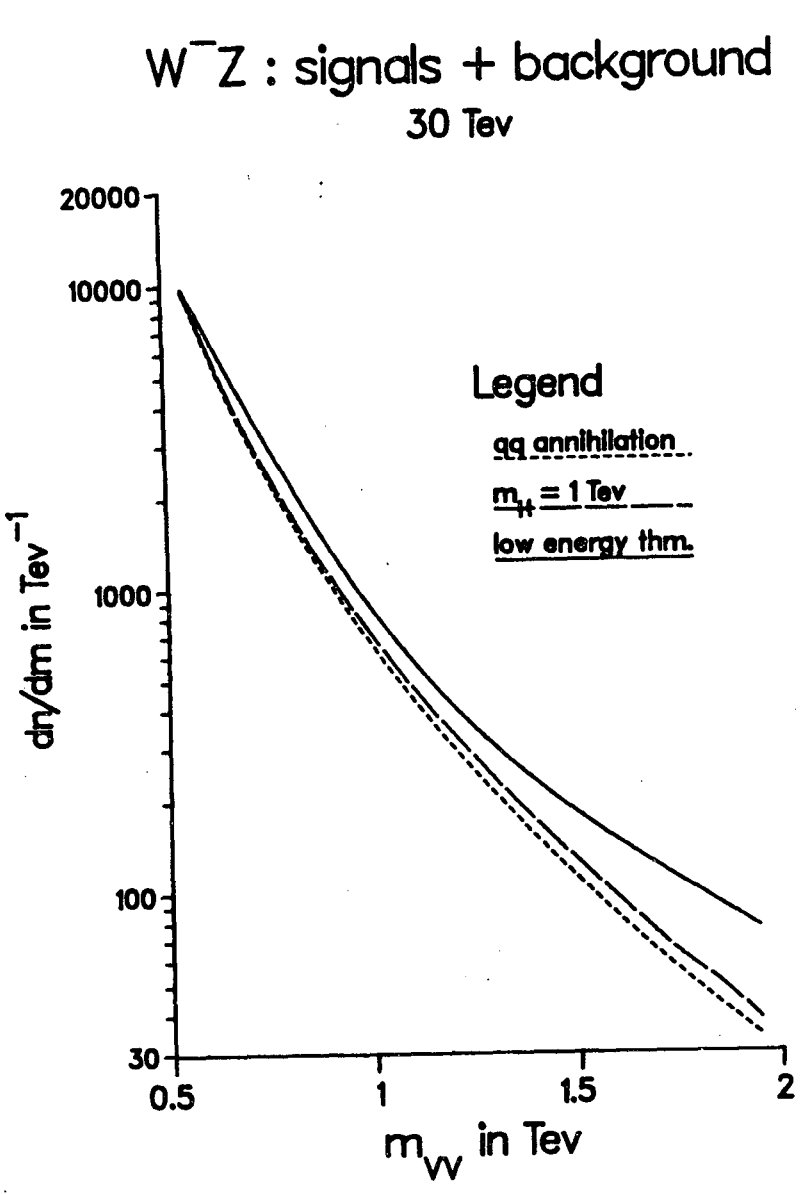

Figure 26

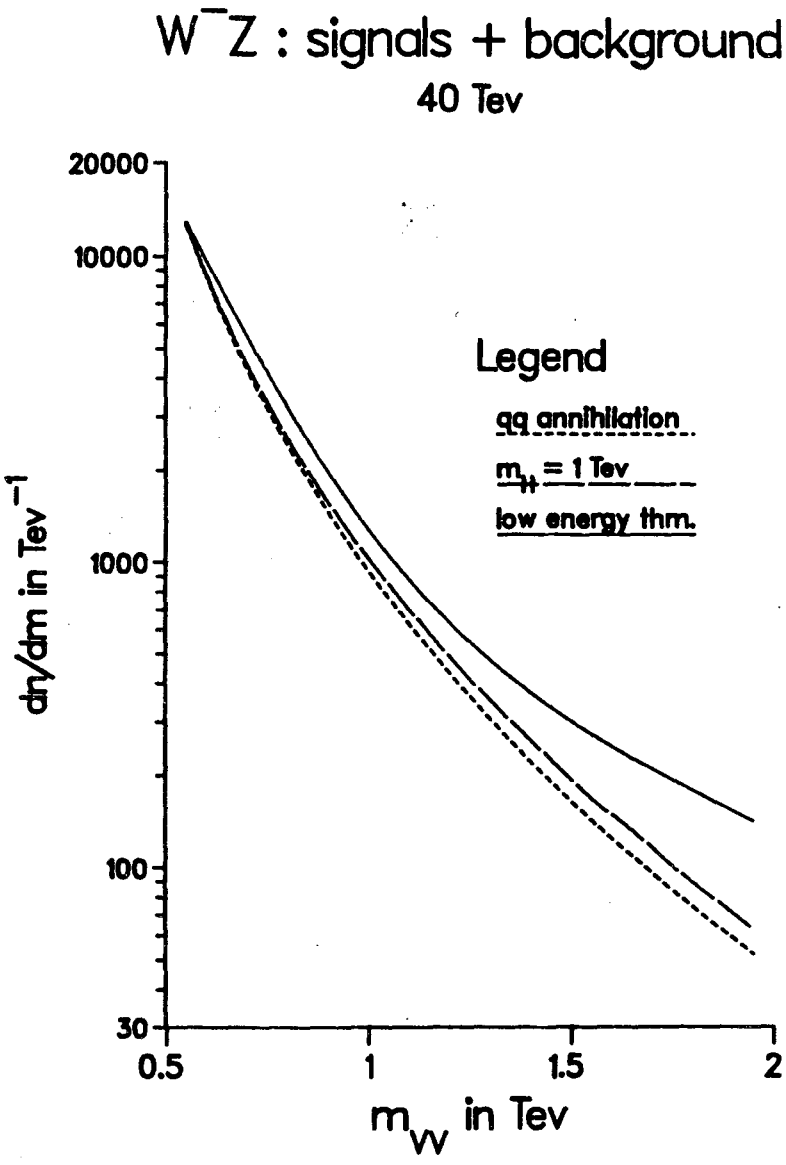

Figure 27

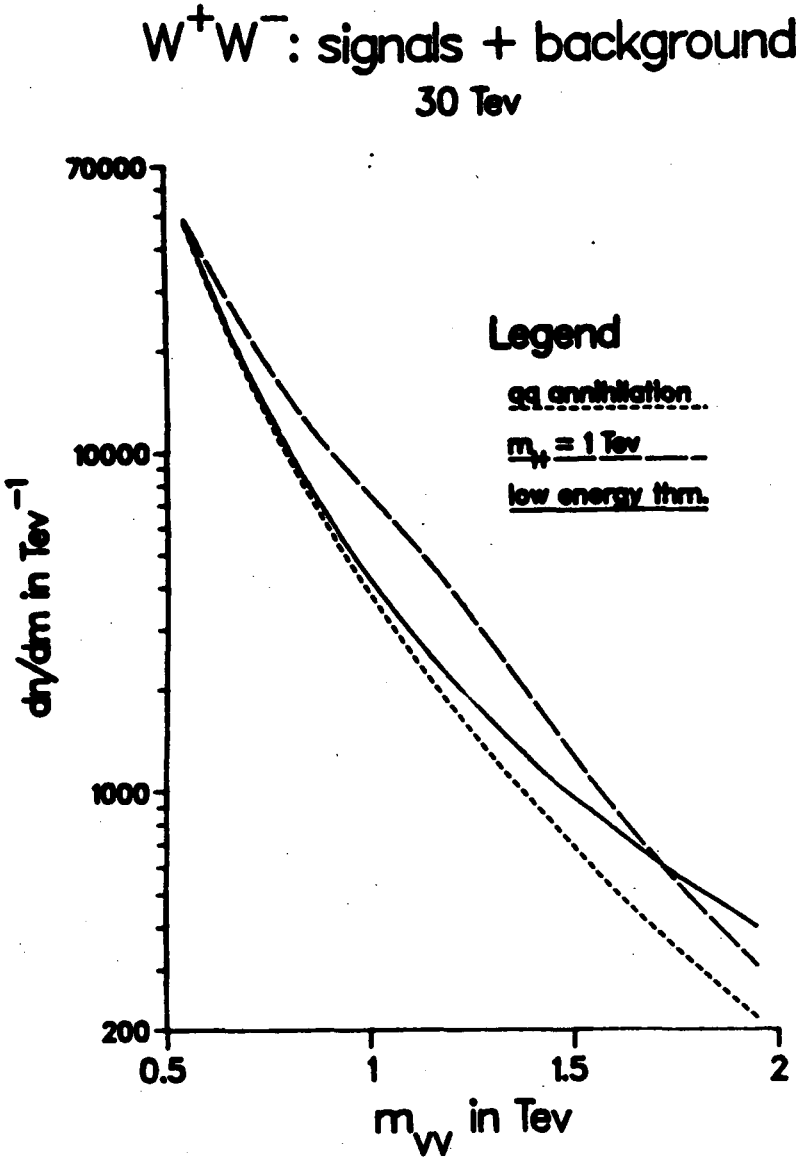

Figure 28

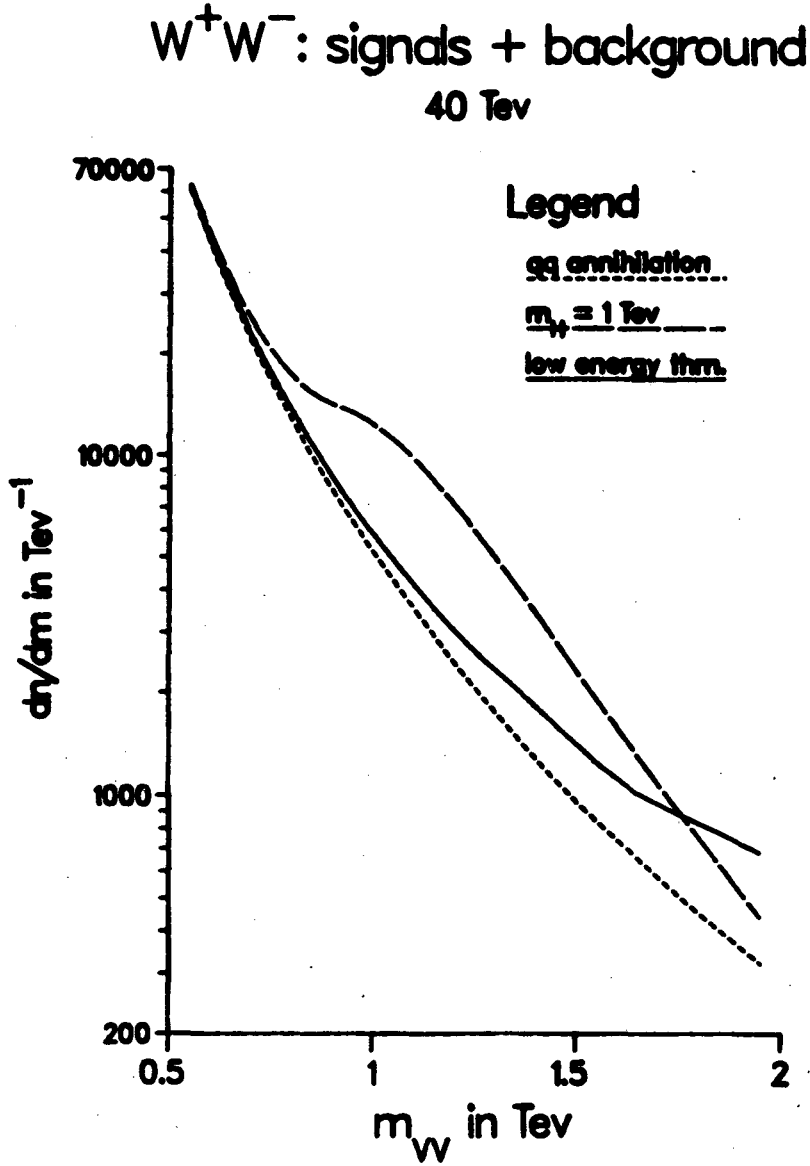

Figure 29

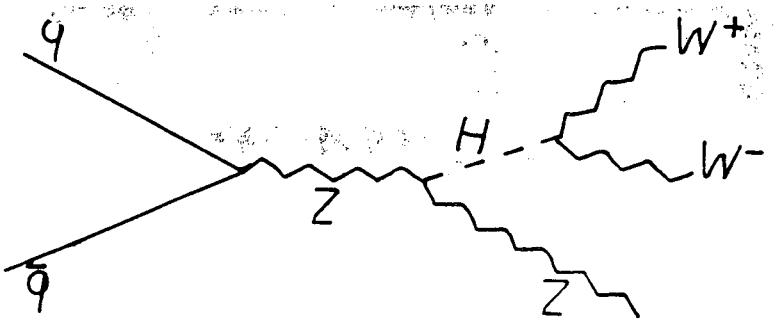

Figure 30

This report was done with support from the Department of Energy. Any conclusions or opinions expressed in this report represent solely those of the author(s) and not necessarily those of The Regents of the University of California, the Lawrence Berkeley Laboratory or the Department of Energy.

Reference to a company or product name does not imply approval or recommendation of the product by the University of California or the U.S. Department of Energy to the exclusion of others that may be suitable.

LAWRENCE BERKELEY LABORATORY
TECHNICAL INFORMATION DEPARTMENT
UNIVERSITY OF CALIFORNIA
BERKELEY, CALIFORNIA 94720